Co-published by
Institute of Fluid-Flow Machinery
Polish Academy of Sciences
Committee on Thermodynamics and Combustion
Polish Academy of Sciences

Copyright©2025 by the Authors under licence CC BY-NC-ND 4.0

http://www.imp.gda.pl/archives-of-thermodynamics/

ARCHIVES OF THERMODYNAMICS

Steam and gas microturbines. Overview

Krzysztof Kosowski[a], Marian Piwowarski[a*], Robert Stępień[b], Wojciech Włodarski[a]

[a]Faculty of Mechanical Engineering and Ship Technology, Gdansk University of Technology, Narutowicza 11/12, 80-233 Gdansk, Poland
[b]Proturb, Poland, Fiszera 14/513, 80-231 Gdansk, Poland
*Corresponding author email: marian.piwowarski@pg.edu.pl

Received: 12.06.2025; revised: 02.09.2025; accepted: 11.09.2025

Abstract

In the contemporary energy landscape, governments are focusing on improving the efficiency of electricity generation and promoting distributed energy systems based on local and renewable sources. This has led to a substantial increase in the number of prosumer, polygeneration, and microgeneration power plants currently under development. In the case of micro-power plants, often turbine-based, particular emphasis is placed on the durability, reliability, cost-effectiveness, and efficiency of both individual components and the entire system. The construction of microturbine power plants involves several challenges, including component miniaturisation, achieving extremely high rotational speeds, efficient power transmission, maintaining adequate safety standards, reducing noise, minimising emissions of harmful compounds, and designing the electric generator. Additional difficulties concern the optimisation of thermodynamic and fluid-dynamic processes, the high-efficiency design of flow components, ensuring bearing and dynamic stability in high-speed rotating systems, miniaturising heat exchangers, and enhancing thermal processes. Despite the availability of commercial microturbine solutions, recent years have seen intensified research and development efforts. The evolution observed in this field suggests that efforts to improve efficiency, durability, reliability, and cost-effectiveness will continue, strongly supported by government involvement. Current progress and accumulated experience have enabled the development of engineering calculation methods for microturbine design, a crucial element of microgrids. This paper reviews the existing literature on microturbines, with particular attention to experimental results and examples of practical designs. It also outlines the main challenges faced by designers and engineers in developing such systems.

Keywords: Gas microturbines; Steam microturbines; Organic Rankine Cycle; Adhesion turbine

Vol. 46(2025), No. 3, 17–37; doi: 10.24425/ather.2025.154921

Cite this manuscript as: Kosowski, K., Piwowarski, M., Stępień, R., & Włodarski, W. (2025). Steam and gas microturbines. Overview. *Archives of Thermodynamics*, 46(3), 17−37.

1. Introduction

In the current 21st century, there is an increasing prevalence of trends towards miniature engineering. Their presence is evident in a variety of sectors, including the power industry, where they are employed in refrigeration, heat exchange, chemical processes, and power generation processes (microturbines, micropumps, micro-compressors, micro-valves, micro-heat exchangers, micro-motors, etc.) [1–3]. The popularity of microturbines has increased significantly over the past two decades, due to their status as relatively small devices. The characteristics of the devices under discussion are as follows: they are characterised by relatively low electrical power (ranging from 25 to 500 kW), very high rotational speeds (ranging from 50 to 120 000 rpm, with some microturbines reaching speeds of up to 1 million rpm [4,5]), and relatively good efficiencies (ranging from 20% to 30% without regeneration). These devices allow for diversification of the energy source in the region [2,6].

Nomenclature

Abbreviations and Acronyms

ACM – air cycle machine
CBC – closed Brayton cycle
CHP – combined heat and power (system)
EMG – electromagnetic generator
FBG – fibre Bragg grating
GMT – gas microturbine
GWP – global warming potential
HRSG – heat recovery steam generator
LSTM – long short-term memory
MEMS – micro-electro-mechanical systems
NZEB – net zero energy building
ODP – ozone depletion potential
ORC – organic Rankine cycle
OTEC – ocean thermal energy conversion
PLM – porous layer model
STG – steam turbine generator
TENG – triboelectric nanogenerator
VOC – volatile organic compound

The advantage of microturbines is their versatility in terms of fuel selection. In addition to conventional fuels such as natural gas and diesel, microturbines have the capacity to utilise a wide range of alternative fuels, including landfill gas, sewage treatment plant gas, flue gas, coal gasification gas, biofuels, methanol, ethanol, and hydrogen, among others [7].

At present, a significant number of corporations are engaged in conducting extensive research and development projects with the objective of constructing microturbines that exhibit enhanced efficiency, reliability, durability and cost-effectiveness. The primary objective of the activity is to achieve efficiencies in excess of 40%, with a concomitant reduction in NO_x emissions and an increase in availability (continuous operation between overhauls of more than 50000 hours), reducing investment costs (< 500 USD/kW), improving fuel flexibility (the ability to utilise several types of fuel, including biofuels, etc.). It is evident that a significant number of globally renowned corporations are engaged in addressing these issues. While some entities have already commenced the provision of microturbines to the commercial sector, ongoing research in this domain persists, with continual advancements being made. The challenges posed by the miniaturisation of components are manifold. These include, but are not limited to, difficulties with bearing and transmission at very high speeds. In addition, there is a need to ensure a proper level of safety, to reduce noise and to reduce the emission of harmful compounds into the atmosphere. A significant challenge confronting manufacturers pertains to the quality of electric generation, encompassing essential parameters such as required voltages, frequency, and power output, among others. This challenge persists during transient conditions. Concurrently, advanced research is being conducted into the use of new types of materials (synthetics, composites, ceramics, aluminium alloys, etc.) [8,9].

In the domain of micro systems, the primary concern pertains to the overall dimensions of the system. Miniaturisation facilitates the acquisition of information with greater efficiency, thereby reducing the material and energy requirements during the production process. Intelligent microsystems, equipped with microsensors and actuators, possess the capacity to interact with their environment and respond to changes therein. The utilisation of micro power supplies and microelectronics for signal processing is a prerequisite for such systems. The integration of these components enhances system efficiency, resulting in faster, more reliable, and cost-effective operation, while concurrently reducing power consumption and enabling the execution of more complex functions [10,11].

In the last two decades, there has been a marked increase in the number of articles dealing with microturbines, as evidenced by data from Elsevier's electronic journal database, which is available through the ScienceDirect platform (Fig.1).

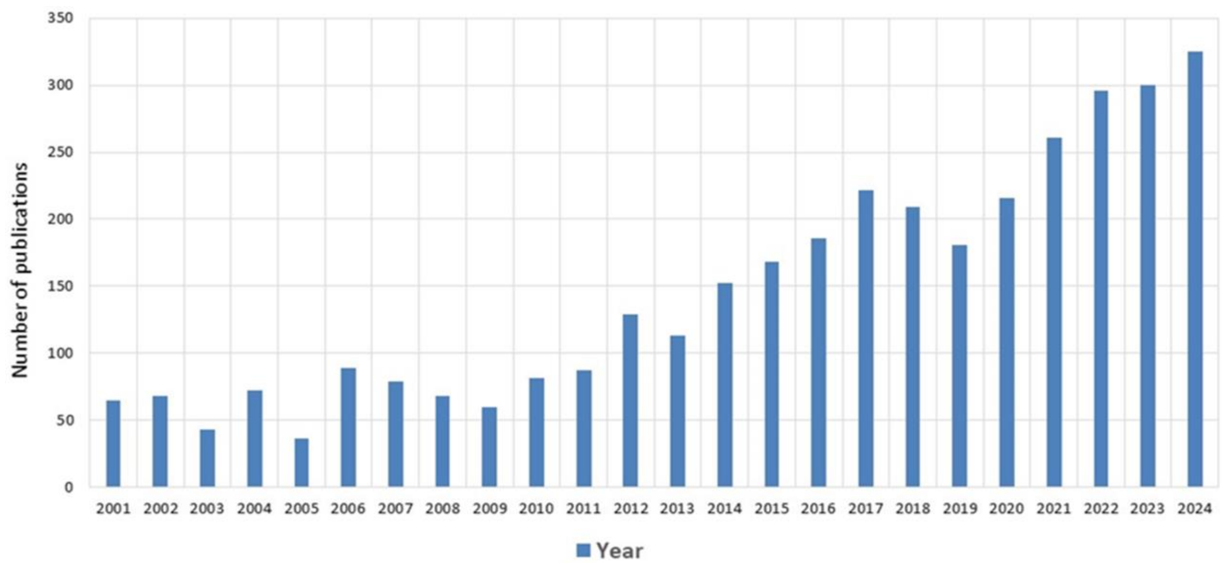

Fig. 1. Number of publications on microturbines from Elsevier's electronic journals database.

The objective of this paper is twofold: firstly, to present and systematise extant solutions for vapour and gas microturbines; and secondly, to explore the potential for future development in this area. The analyses were conducted using a range of academic databases, including Elsevier Open Access, Institute of Electrical and Electronics Engineers, and Springer, to name a few. In certain instances, the authors have encountered difficulties in accessing more detailed information due to the protection of intellectual property rights. The paper is organised into five main chapters, with each one focusing on specific aspects of these solutions. Vapour microturbines are categorised into two types: those using steam as the working medium (Rankine cycle) and those employing other working media in the Organic Rankine Cycle (ORC). The latter type of micro power plant, in particular, is undergoing significant development. The next chapter discusses gas microturbines, which are also experiencing rapid advancements. A separate chapter is dedicated to Tesla microturbines, given their ability to utilise various working media, including steam, organic vapour, air, or flue gases, which complicates their classification within a single category. Additionally, a chapter has been dedicated to microturbines (both steam and gas) that employ Microelectro-Mechanical System (MEMS) technology, in addition to the analyses presented in other chapters.

2. Steam microturbines

Steam turbines are among the most versatile and long-standing prime mover technologies still widely used today. The utilisation of steam turbines for power generation has a long history, having replaced reciprocating steam engines due to their superior efficiency and lower costs. In the extant literature, steam microturbines are referred to as devices that produce energy measured in kilowatts or even watts. Up to now, quite a few power stations have been equipped with steam microturbines. However, this knowledge and technology domain is still dynamically developing, in a similar manner to gas microturbines. The advantages of the steam microturbine are:

- a proven technology,
- broad power range,
- acceptable efficiencies (at least at nominal conditions),
- separation between combustion and power generation.

The main disadvantages are:

- low efficiency at partial load,
- relatively high costs for a small size [8].

The Rankine cycle is the most common thermodynamic cycle employed in steam turbines. This cycle constitutes the fundamental principle underlying conventional power-generating stations, Fig. 2, and it is realised in four ideal thermal processes [6]:

- heat supply at constant pressure (usually, in the boiler furnace, due to chemical reactions of fuel combustion, heat is generated and used for changing the water into steam, most frequently superheated),
- isentropic expansion (the steam of high pressure and temperature generated in the boiler enters the turbine where it expands to the low pressure of the condenser),
- heat rejection at constant pressure (in the condenser, the steam rejects its heat of condensation to a cooling system),
- isentropic compression (in the pump, the isentropic process of compression takes place, transforming the water from saturated liquid state to feed water at high pressure).

The steam microturbine has also been incorporated into hybrid cogeneration, trigeneration and combined steam-gas power systems [12].

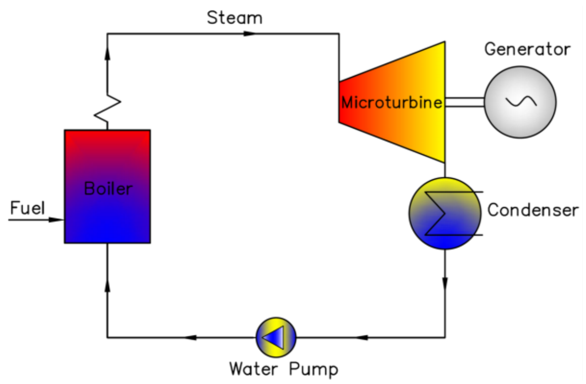

Fig. 2. Diagram of a steam microturbine cycle.

An example of a steam microturbine set is shown in Fig. 3 [13]. The Steam Turbine Generator (STG) system consists of a high-speed steam microturbine with an axial inlet and radial outlet with a high internal efficiency of 80%, a planetary gearbox reducing the speed in a ratio of 7.78:1 and a generator with efficiency above 95%. The efficiency depends on the parameters of the inlet steam. It has been demonstrated that the turbine set has the capacity to generate 275 kW of electrical power [14]. The centrifugal microturbine used in this solution allows large enthalpy drops to be realised with good efficiency at low mass flow rates.

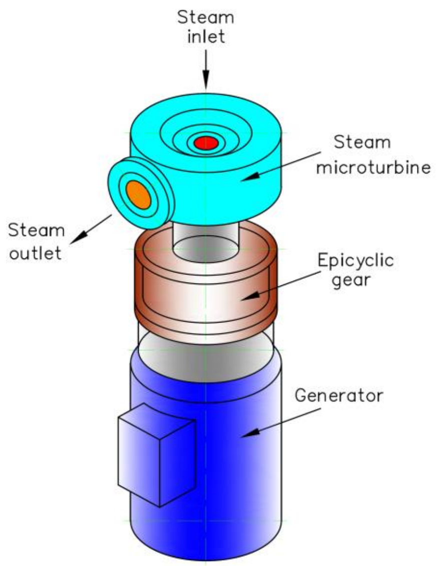

Fig. 3. Steam microturbine model STG.

In 2004, a prototype of a gas-powered domestic SteamCell unit for combined heat and power generation based on a steam unit was presented (Fig. 4) with an efficiency of 25%. The system has been demonstrated to deliver a range of electricity outputs between 0.5 kW and 4.6 kW, in conjunction with heat outputs ranging from 2 kW to 25 kW. In this particular instance, the conventional Rankine cycle is augmented by the incorporation of an additional domestic water heater [15].

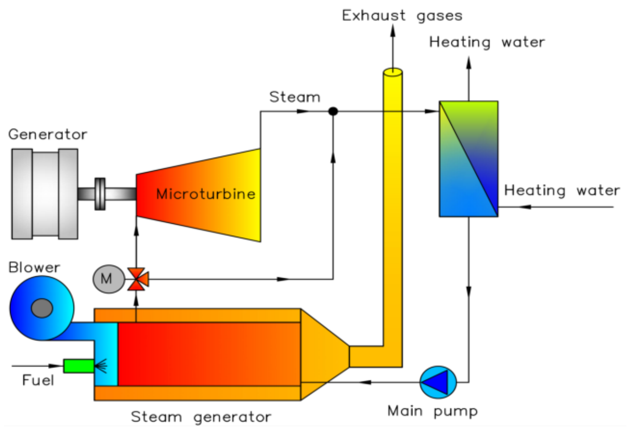

Fig. 4. Functional diagram of the SteamCell system.

The paper [16] presents a two-stream flow centripetal microturbine. The unit's maximum electrical power output is 50 kW at 12 000 rpm. The rotor is supported by rolling bearings. In experimental tests for an inlet steam pressure of 0.6 MPa, temperature of 159°C and mass flow rate of 0.21 kg/s, 30.37 kW of electrical power was obtained.

Another example of a steam turbine test rig is the system that was installed at the Maine Maritime Academy[17]. The facility has two steam turbine units. One is a single-stage Curtis turbine, and the other is a multi-stage axial turbine. Operation parameters: outlet pressure of 800 kPa, outlet temperature of 289°C, boiler inlet water temperature of 63°C, condenser pressure of 20 kPa, turbine outlet temperature of 110°C (Curtis stage) and 60.1°C (multi-stage turbine), rotational speed of 3 600 rpm, electric power of 8.21 kW (Curtis stage) and 13.32 kW (multi-stage turbine), with overall circuit efficiency of 11.4% (Curtis stage) and 18.55% (multi-stage turbine). There are some disadvantages to both solutions. The Curtis turbine stage is less efficient, and the multistage turbine is more complicated.

The New England Steam Turbine Corporation, on the other hand, makes NESTCO N17 H single-stage steam turbine units. These have a power output of 1260 hp (≈940 kW), an inlet steam temperature of 440°C, a pressure of 49 bar and a speed of 6 300 rpm. This is also a Curtis turbine stage device. The company also offers a vertical-flow version of the NESTCO N17 V microturbine. Both devices are used to drive pumps [18].

Another intriguing steam microturbine solution is a counter-rotation turbine with two separate rotors, without a stator between them, rotating in opposite directions, driving two separate high-speed permanent magnet generators (see Fig. 5). Figure 5a presents a microturbine set, while Fig. 5b shows a partially decomposed device with visible separate rotor blade cascades. It is a device that uses the summation of velocity vectors resulting from the modification of the Ljungström turbine. The microturbine has been demonstrated to facilitate a power output of approximately 1,5 kW at an inlet steam pressure of around 5 bar, a temperature of approximately 220°C, and outlet parameters of 10 kPa and 40°C. These conditions are maintained while the microturbine operates at a rotational speed of 30 000 rpm and a mass flow rate of 5 g/s. This approach has been patented [19] and has undergone theoretical testing and analysis. The feasibility of a compact design that is capable of effective electricity production was demonstrated [20,21].

a) b)

Fig. 5. View of a steam microturbine with two generators (a) and both counter-rotating rotors in separate housings (b).

For example, in Russian developments led by the Don Technologies consortium, single-stage, two-flow active centripetal steam microturbines have been applied, operating in the range of 30–50 kW electric power and up to 600 kW thermal power. Their design enables independent regulation of electricity and heat generation, which distinguishes them from gas turbine and piston units. Experimental investigations, however, revealed the need for further optimisation of blade profiles and reduction of efficiency losses during wet steam operation [22].

In studies on cogeneration systems, integrating gas and steam microturbines with ORC loops and solar collectors has been emphasised. Advanced concepts couple a microturbine with a parabolic dish collector and a Brayton cycle, while waste heat recovery is performed through dual-stage ORC modules. Such configurations significantly improve exergy efficiency and reduce fuel consumption, achieving overall efficiencies exceeding 70% [23].

Although steam microturbines were not the primary focus in research on building-integrated nanogrid systems, they are often discussed in the broader context of decentralised trigeneration. Integration of microturbines with thermal energy storage highlights their potential use in Net Zero Energy Buildings (NZEBs), where they can complement renewable sources and support local heating and cooling demands [24].

Another promising direction is the application of microturbines in mobile and transport energy systems. Research on sustainable tramway power supply has demonstrated the feasibility of integrating microturbines with biomass gasifiers. In such configurations, microturbines act as stabilising units for the entire energy system, working in conjunction with energy storage and renewable sources, thereby enhancing energy autonomy and reducing CO_2 emissions [25].

Utilising the microturbine configuration presented in Fig. 5, the authors have proposed a solution for a steam micro-turbine that operates in an emission-free mode. This solution involves the combustion of hydrogen in an oxygen, resulting in the generation of steam as the working medium. The concept of such an installation is illustrated in Fig. 6, while the test stand is presented in Fig. 7. The proposed solution is straightforward and analogous to the Rankine system. The hydrogen burner generates high-temperature steam. The process of steam generation at a lower temperature, permissible for the turbine, is achieved by the supply of water to the burner. Steam expands in the turbine and is then condensed in a water-cooled condenser. The work of the turbine is used to produce electricity in the generator.

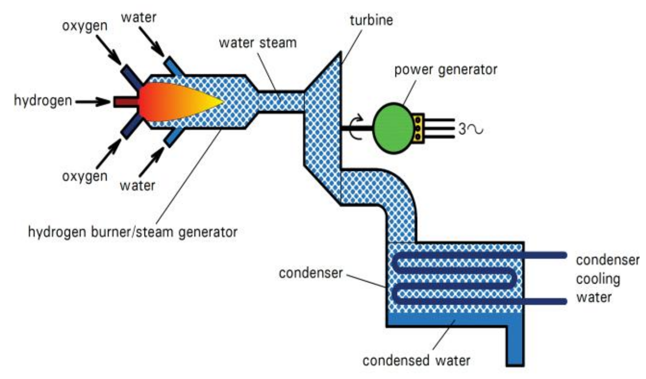

Fig. 6. Concept of operation of a hydrogen microturbine.

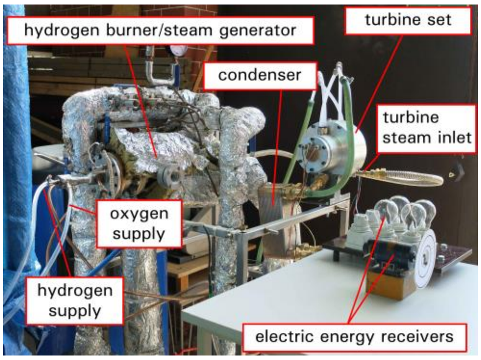

Fig. 7. View of the hydrogen microturbine test stand.

In addition to the commercial versions, laboratory-scale stations are also available. The steam parameters at the boiler outlet are a pressure of 827 kPa and a temperature of 250°C, and the resulting electrical power is approximately 15 W [26]. These are student stands designed to present the idea of the Rankine cycle.

In this chapter, the authors have conducted a review of extant design solutions for microturbines with steam as the working medium. Although few examples of steam-based microturbines have been cited, their development is ongoing. Steam microturbines have very low steam flow rates and high enthalpy drops, so special designs must be used to achieve good efficiency. A range of adaptations have been derived from high-power steam turbine solutions, including multi-stage axial micro-turbines, micro-turbines with Curtis stage, centripetal turbines, and turbines with contra-rotating rotors. Each of these has its own advantages and disadvantages, and ongoing development is focused on enhancing efficiency, durability, and reliability. However, recent trends in micro turbine development appear to be shifting towards the utilisation of working media other than water. These are ORC cycles, which will be discussed in more detail in the next chapter.

3. Microturbines in ORC cycles

The fundamental operating principle of ORC technology was first established in 1826 by Howard. He used ether as the working medium. It was not until more than a century later that D'Amelio constructed an ORC power plant in 1936, equipped with a single-stage impulse turbine and monochloroethane (C_2H_5Cl) as the working medium, heated by solar energy. Subsequently, during the 1960s, research into potential working fluids was initiated, which led to the identification of the advantages of chlorofluorocarbons (CFC) use and the establishment of the ORC cycle with regeneration. This cycle continues to be utilised extensively in the present day. This development subsequently prompted the conception of multiple prototypes by ORMAT in 1964 and Turboden in 1970. These enterprises have since emerged as the foremost entities within the ORC market [27].

The initial ORC systems, which were in operation between 1960 and 1980, are summarised in Table 1.

Table 1. First ORC systems built between 1960 and 1980.

Year	Power, kW	Working fluid	Temperature, °C	Pressure, bar	Number of systems	Country
1961	347	R11	-	-	1	USA
1966	190	R11	120	12,5	1	Japan
1967	750	R12	-	-	1	USSR
1968	3800	R11	121	12,8	1	Japan
1969	475	R11	116	11,6	1	Japan
1972	108	Fluorinol 85	288	48,3	1	USA
1974	500	R11	123	13,3	1	Japan
1975	600	Toluen	274	22	1	USA
1977	500	R113	90	12,4	1	Japan
1977	34	Fluorinol 50	321	55,2	1	USA
1978–1982	600	Toluen	251–274	16–22	5	USA
1979	200	Toluen	-	-	1	USA
1979	40	Tetrachloroethylen	110	0,7	1	Italy
1979	500	R11	88	6,2	1	USA
1979	21	R114	92	-	1	Germany
1979	100	Toluen	320	-	1	Germany
1979	170	Toluen	323	-	1	Germany
1979	500	R114	85	-	1	Germany
1979	30	R11	160	13	1	Germany
1980	45	C_8F_{16}	280	11,6	1	Italy
1980–1983	50–600	R114	-	-	22	Israel
1981	14000	Fluorinol 85	260	34	1	Japan
1981–1984	1000–1500	R113	130	7,9	3	USA
1982	130	R11	-	24	1	Germany
1982	500	R114	105	15,3	1	Italy
1982	5000	R114	75	8,1	1	USA
1983	1000	Fluorinol 85	330	50	1	France
1983	3280	R11	90	6,7	1	Japan
1984	100	Dichlorobenzen	173	0,9	1	Italy
1984	100	C_8H_{10}	130	0,8	1	Italy
1984	100	R114	170	22	1	Finland

The assembly of these power plants was primarily undertaken in the USA, Japan, Germany, Israel and Italy, with capacities ranging from a few tens of kilowatts to several megawatts. A solution with a capacity of up to 1 MW can be designated as a microturbine unit. At that time, the following refrigerants were typically utilised: R11, R12, R113, R114 and Fluorinol [7,28].

We can see from the table that the temperatures used in those years were quite low. They did not exceed 330°C. On the other hand, the pressures were already above 55 bar. It is generally accepted that steam power plants above 350°C have higher efficiencies than those using organic media [29]. At lower temperatures, thermodynamic cycles using organic fluids can achieve a higher level of efficiency than those using steam [30]. The construction of this type of power plant was later somewhat abandoned, but the last two decades have seen a rapid development of ORC systems and associated microturbine technology.

The ORC is similar to the cycle of a conventional steam turbine, except that the medium that drives the turbine is a high molecular weight organic fluid. The selected working fluids allow efficient use of low temperature heat sources to generate electricity over a wide power range (from a few kW up to 1 MW per unit). The organic working fluid is vaporised in the evaporator, then it expands in the turbine and is then condensed using cooling water in a heat exchanger (alternatively, ambient air can be used for cooling). The condensed medium is then pumped back to the evaporator, and the thermodynamic cycle is closed. Heating and cooling sources are not in direct contact with the working fluid or the turbine. For high temperature applications, e.g. combined heat and power biomass-powered plants, high temperature thermal oil is used as a heat carrier and a regenerator is added to further improve the cycle performance. The main technical advantages of ORC plants are as follows:

- relatively high cycle efficiency for a low value of upper cycle temperature,
- high turbine efficiency (up to 85%),
- no erosion of blades, due to the absence of moisture,
- long life time,
- no operator is required.

The system also has practical advantages, such as simple start-stop operation, quiet operation, minimum maintenance requirements, and good part load performance. Typical applications are:

- power plants with low temperature geothermal fluids, up to 1 MW electrical power per unit,
- biomass fueled plants,
- heat recovery applications (in the range of 400 to 1500 kW electrical power),
- solar systems application [31].

Many companies have developed and implemented their own technologies in recent years, e.g. radial flow turbines, axial microturbines, direct evaporation turbine units, centripetal radial flow microturbines or screw expanders [27,28]. By the end of 2016, 1754 ORC turbine units with a total installed capacity of more than 2.7 GW had been built, according to the study [27].

Often the main source of energy in ORC power plants is waste heat from various energy, industrial, agricultural or even domestic processes [32,33]. The utilisation of this particular type of heat facilitates enhanced energy efficiency by means of its recovery and reuse, as opposed to its dissipation into the environment. To illustrate, in industrial facilities such as steel mills, cement plants and chemical plants, waste heat is frequently a by-product of technological processes [34,35]. Numerous examples in the extant literature illustrate the utilisation of waste heat from internal combustion engines [36] as well as from gas turbines [37] as a source of thermal energy for ORC systems. The implementation of these solutions has the potential to enhance the overall energy efficiency of these units, which, in practical terms, is evidenced by a reduction in energy losses and an increase in efficiency by several percentage points.

In addition to waste heat, geothermal energy is a frequently analysed and utilised energy source for ORC systems [38]. Geothermal heat sources, including hot springs and geothermal boreholes, are a stable and renewable energy source that can power ORC power plants throughout the year, irrespective of weather conditions. Another area of interest is the use of solar energy [39], which, when utilising suitable solar collector technology, can be efficiently converted to thermal energy to power the ORC cycle. In coastal or island regions, examples are also emerging of the use of ocean thermal energy, known as Ocean Thermal Energy Conversion (OTEC) energy, as a heat source for ORC power plants [40]. This type of solution is based on the temperature difference between the warmer surface of the ocean and the cooler layers of the deep sea, making it possible to generate electricity in a renewable and environmentally friendly manner. The above-mentioned heat sources vary considerably in temperature from around 30°C to 200°C, which has a significant impact on the selection of working medium and, consequently, the design of the microturbine.

The working fluids utilised in ORC power plants are required to adhere to a multitude of criteria, which poses a significant challenge in the design of such systems. Operational safety is paramount, necessitating the use of a working fluid that exhibits minimal toxicity and environmental impact. In practice, substances with high greenhouse gas potential (GWP) and high ozone depletion potential (ODP) are typically excluded or used only in exceptional cases. The environmental impact of a given substance is also associated with its capacity for biodegradation and the emission of volatile organic compounds (VOCs). In addition to the environmental aspects, the working fluid should be inexpensive and readily available on the market. The cost of the working fluid has a direct impact on the cost-effectiveness of the overall project, particularly in the case of larger installations, where the quantity of fluid required is substantial. Another important requirement is its chemical stability, both thermal and material. It is imperative that the working medium does not react chemically with the components of the flow system (e.g. heat exchangers, turbines or piping), as this could lead to their corrosion or degradation and, consequently, result in the premature failure of the plant. In practice, it is often challenging to identify a working medium that fulfils all these requirements while preserving optimal thermodynamic properties. Consequently, designers are compelled to make compromises, which may entail the implementation of more sophisticated and costly safety technologies, such as leak detection systems or fire protection systems, particularly in the context of flammable media, including saturated hydrocarbons (methane, propane) and unsaturated hydrocarbons (ethane, ethylene). It is therefore evident that the selection of the operating medium constitutes a significant engineering challenge in the design of ORC systems, given the extensive range of potential substances that can be utilised.

The extant literature comprises analyses of diverse groups of compounds, including saturated hydrocarbons (e.g. n-pentane), unsaturated hydrocarbons (e.g. propylene), cyclic hydrocarbons (e.g. cyclohexane), heterocyclic hydrocarbons (e.g. furfural), aromatic hydrocarbons (e.g. toluene), as well as synthetic refrigerants (R134a, R1234yf), alcohols (ethanol, methanol), siloxanes (e.g. MM, MD2M) and other compounds [41]. A number of studies have been conducted on the selection of suitable operating agents for ORC systems, as it is crucial for process efficiency and stability. A range of studies have been conducted that consider both synthetic refrigerants and natural organic compounds with a view to determining whether they can meet the requirements of specific applications. The most commonly used working refrigerants include compounds such as R245fa, R123, n-butane, n-pentane and R1234yf [41]. These refrigerants possess relatively low boiling points, rendering them efficacious in ORC systems with low to medium heat source temperatures.

Ethanol, as an example of alcohol, is also used as a working fluid in ORC systems due to its thermodynamic properties and relatively low toxicity [40]. Other refrigerants, such as R134a, R152a, R236fa, R245fa, or mixtures such as R404a and SES36, have also been extensively studied in the context of ORC engine applications [37]. Many of these compounds have low ozone depletion potential (ODP) and moderate global warming potential (GWP), making them more environmentally friendly [42,43].

In the context of high-temperature ORC systems, compounds with higher boiling points, such as toluene, siloxanes (e.g. MDM, MM, MD2M), are often preferred [44], which show stability in higher temperature ranges. Furthermore, agents such as ammonia, cyclohexane or acetone are of interest in this context [45], which, due to their chemical and thermodynamic properties, can be used under more demanding conditions, e.g. using waste heat from higher temperature processes.

In the case of some ORC systems, mixtures of operating media are also considered. These mixtures may provide enhanced thermodynamic properties, but their composition and characteristics are often not commercially available and, in many cases, are protected by patents. Therefore, the selection of a suitable working medium should prioritise cycle efficiency and maximise the use of the available heat source, which directly affects the energy efficiency of the overall system.

A fundamental difference between ORC cycles and conventional Rankine cycles lies in the temperature of the working medium at the turbine inlet. This results from the specific properties of the organic fluids employed, such as isopentane, R245fa, or siloxanes. These fluids have a lower evaporation temperature than water, enabling the efficient utilisation of low- and medium-temperature heat sources. Consequently, conventional ORC power plants typically achieve efficiencies in the range of 10−12%, while modified ORC systems can reach efficiencies of up to 15−20% [46]. Such modifications may include an increase in the maximum temperature or a change in the structure of the entire plant. Increasing the temperature of the working medium at the turbine inlet leads to a higher temperature difference over the cycle and, consequently, an increase in thermodynamic efficiency [47]. This is achieved by using stronger materials in heat exchangers and turbines, allowing for safe operation at higher temperatures. Another method of increasing efficiency is to modify the plant structure. The incorporation of an additional cycle is an illustrative example of the concept, as it results in the establishment of a cascade system. In such a system, the waste heat from the first cycle is utilised as a heat source for the second cycle, which results in a substantial increase in the overall efficiency of the plant [48].

In addition, the implementation of an auxiliary heater has been demonstrated to enhance the temperature of the working medium prior to its expansion within the turbine, thus leading to an enhancement in process efficiency [49].

As in conventional steam turbine systems, the efficiency of ORC cycles can also be increased by using an interstage superheater. Interstage superheating entails heating the medium after partial expansion in the turbine, which enhances the efficiency of subsequent expansion [50]. Moreover, the utilisation of regenerators facilitates the recovery of heat from the working medium following expansion. This process elevates the temperature of the medium prior to its entry into the evaporator, thereby diminishing the heat demand [51,52].

Another modification that has the potential to enhance efficiency is the implementation of a parallel evaporator. This apparatus facilitates the concurrent utilisation of diverse heat sources, each with distinct parameters. Consequently, it enables the optimised alignment of the cycle's properties with the available resources, thereby ensuring enhanced efficiency [53].

In addition to structural changes, efficiency improvements can also be achieved by optimising the operation of individual power plant components such as turbines, compressors, boilers, pumps and electrical generators. The optimisation of turbines and compressors through the utilisation of contemporary materials and precision machining technologies has been demonstrated to reduce mechanical losses and enhance efficiency. Improvements to heat exchangers, such as boilers and evaporators, can increase the efficiency of heat transfer. Moreover, modern electric generators with higher efficiency allow for better conversion of mechanical energy into electricity.

Nevertheless, despite these advances, a significant disparity in efficiency persists between ORC systems and conventional steam or gas cycles. Consequently, there is an ongoing focus on research endeavours aimed at enhancing the efficiency of ORC power plants. A pivotal advancement is the augmentation of working fluid parameters, including temperature and pressure. New working fluids with higher thermal stability can enable operation at higher temperatures, which would significantly increase cycle efficiency. Concepts such as Kalina cycles and supercritical ORCs represent promising research directions, as they offer the potential to achieve higher efficiencies by better matching the properties of the working fluid with the available heat sources [54,55].

The development of ORC microturbine design focuses both on enhancing flow efficiency and minimising losses, as well as ensuring operational reliability. Of particular importance are sealing solutions aimed at reducing working fluid leakage. In addition to conventional labyrinth seals, honeycomb-type seals have been investigated, which effectively reduce leakage flows but require advanced manufacturing technology and may introduce additional frictional losses [56]. In parallel, experimental studies of microturbogenerators have demonstrated the existence of optimal heat source power and generator load values at which maximum electrical output can be achieved [57].

Another crucial direction of development is the implementation of advanced diagnostic and condition monitoring systems. Fibre Bragg Grating (FBG) optical sensors enable leakage detection and temperature monitoring of critical microturbine components [58], while artificial intelligence algorithms, such as Bayesian-optimised Long Short-Term Memory (LSTM) networks, allow rapid identification of sensor malfunctions, thereby improving the safety and reliability of ORC systems [59].

As previously stated, the implementation of supercritical parameters has been demonstrated to enhance the efficiency of ORC cycles. However, it has been demonstrated that replacing adiabatic expansion with isothermal expansion can lead to an enhancement in efficiency of up to ten percentage points (see Fig. 8) [47,60].

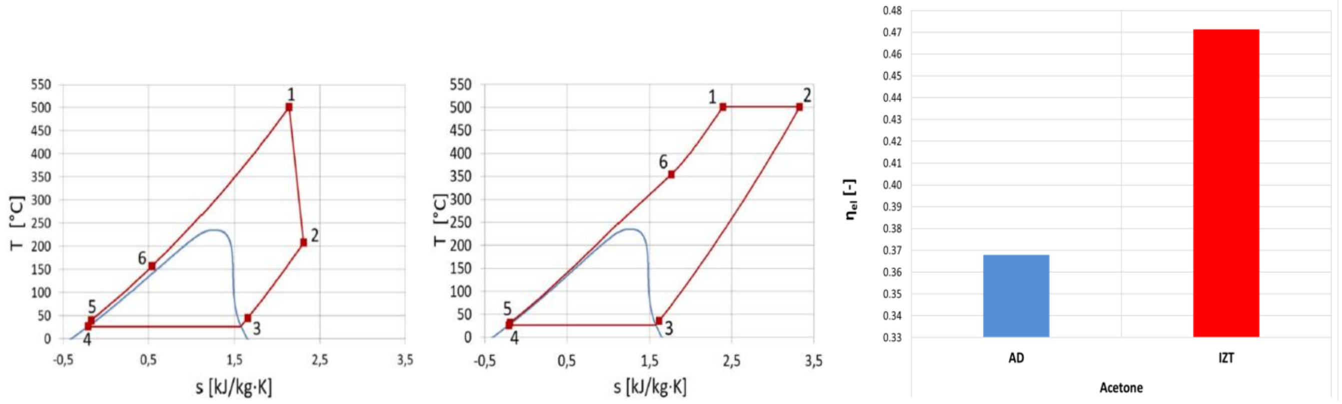

Fig. 8. Thermodynamic cycle of the ORC power plant with acetone as a working medium: (a) adiabatic expansion in the turbine, (b) isothermal expansion in the turbine, (c) comparison of electrical efficiency (AD – adiabatic expansion, IZT - isothermal expansion).

Moreover, endeavours are currently being undertaken to engineer more robust materials for heat exchangers and turbines that have the capacity to function at elevated pressures. This development has the potential to enhance efficiency.

This section of the paper provides a comprehensive overview of the current state of ORC technology. It places particular emphasis on the operating medium, temperature and pressure levels, as well as the specifics of each application, which are primarily influenced by the heat source. The investigation identified the type of working medium and the turbine as two key aspects of ORC technology. A comprehensive literature review has identified numerous studies addressing working fluids, underscoring their various limitations. The emphasis placed on design solutions by designers and constructors is notable for its simplicity, with axial or radial single-stage turbines being of particular interest. These turbines are characterised by their relatively high efficiency, durability and cost-effectiveness. However, it should be noted here that each case should be treated individually in the design of an ORC micro-turbine, depending on the operating parameters, heat source, intended use and other technological aspects. The primary technological characteristics of ORC solutions were enumerated, and a comparison with the conventional steam cycle demonstrated that ORC systems were more appropriate for low-power (microturbines) and low-temperature applications. The subsequent chapter will address gas microturbines, which are also undergoing development.

4. Gas microturbines

Various configurations of gas microturbine systems have been documented in the existing literature. In the majority of cases, two distinct microturbine power plant schemes are employed: an open cycle scheme (Fig. 9a) and a closed cycle scheme (Fig. 9b). The majority of systems incorporate a recuperator, the function of which is to recover a portion of the exhaust heat. This heat is then utilised to preheat the combustion air (see Figs. 9c and 9d). As demonstrated in Fig. 9c, the air is compressed in the compression section, subsequently mixed with fuel, and then burned to generate power for the turbine section [61].

Gas microturbines are typically fuelled with natural gas, with a generation capacity ranging from 25 kW to 500 kW of electricity. The rotational speed of these engines is notably high, ranging from 50 000 rpm to 120 000 rpm, and occasionally exceeding 100 000 rpm. Their thermal efficiency, ranging from 20% to 30% without regeneration, is considered acceptable. However, with regeneration, the efficiency can be further enhanced. The provision of a diverse energy source within a specific region is facilitated by this mechanism. Gas microturbines are advantageous due to their compact size and relatively low investment cost. Furthermore, the emission levels exhibited during operation are minimal. It is evident that they serve to minimise the ecological impact of substantial transmission and distribution systems. In the contemporary business environment, a significant number of companies are engaged in extensive research and development initiatives related to the construction of gas microturbines. The primary objective of these endeavours is to enhance the efficiency, reliability and durability of these devices, while concurrently reducing their overall cost. The primary objective of these activities is to enhance the effective efficiency, whilst concomitantly reducing NO_x emissions, extending the time between successive overhauls beyond 45 000 hours, and minimising investment costs to below 500 USD/kW. Another issue that must be addressed is the necessity for greater flexibility with regard to the type of fuel utilised. This would entail the use of different fuels for the same turbine, with a particular emphasis on the use of biofuel.

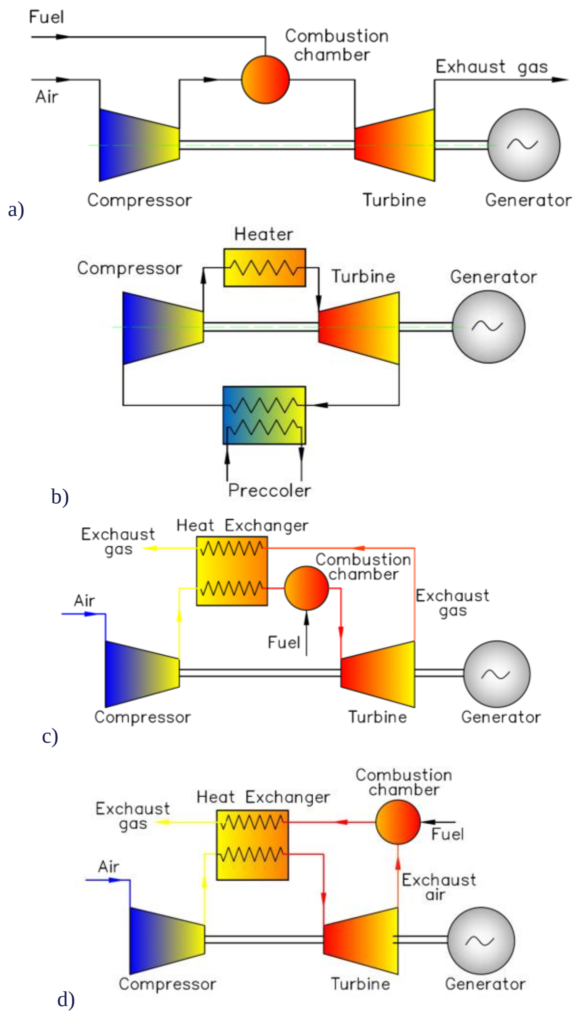

Fig. 9. Open cycle (a) and closed cycle (b) gas microturbine plant. Single shaft open cycle gas microturbines with a heat exchanger and a classical (c) or external (d) combustion chamber.

The majority of manufacturers are adopting a single-shaft design, whereby the compressor, turbine, and permanent-magnet generator are mounted on a single shaft supported by lubrication-free air bearings. These turbines are capable of operating at speeds of up to 120 000 rpm and are powered by natural gas, gasoline, diesel, and alcohol. The dual shaft design incorporates a power turbine and gear for mechanical drive applications and operates up to a speed of 40 000 rpm. The compact and lightweight design of microturbines renders them a viable option for a wide range of light commercial and industrial applications [62].

In industrial practice, gas microturbines (GMTs) are increasingly employed as prime movers in combined heat and power (CHP) systems, simultaneously generating electricity and heat with overall efficiencies of 80–90%. Their advantages include fuel flexibility—from natural gas to biogas—and very low exhaust emissions. Feasibility studies, such as those conducted for industrial laundries, confirm the high economic viability of GMT-based installations as well as significant primary energy savings [63].

As previously stated, a salient benefit of gas microturbines is their capacity to operate on a range of fuels e.g. natural gas, biogas, sewage gas, waste gas, stack gas, gas produced as products of carbon gasification or pyrolysis processes, biofuel, diesel fuel, gasoline, heating oil, methanol, ethanol, propane, hydrogen, etc. Microturbines produce thermal output at a temperature range between 200°C to 350°C, suitable for supplying various thermal needs. Their life time is estimated in the range of 40 000 to 80 000 hours. To date, these units have exhibited adequate reliability. However, not enough time has passed for them to be included in commercial services. As a result, providing data on their entire lifetime is currently unfeasible. Microturbine sets can be connected in parallel to support larger loads and improve power reliability. Reducing the output power of microturbines leads to lower mass flow and combustion temperature; consequently, the efficiency at part load may drop below the design value. Single-shaft gas microturbines with air bearings do not require lubricating oil or water, resulting in lower maintenance costs compared to conventional gas turbines. Microturbines that use lubricating oil do not need frequent oil changes because the oil is kept separate from the combustion products [64].

A distributed power generation system covers a variety of generating technologies, and in addition to microturbines, it includes fuel cells, wind turbines, photovoltaic cells, Stirling engines and internal combustion engines. The main advantages of a distributed power generation system are reducing transmission losses, distributing costs, ensuring higher reliability (especially in smaller systems), and potentially achieving greater overall efficiency by utilising waste heat for cogeneration. While the potential market for microturbines remains uncertain, propane-fueled microturbines offer significant advantages. Propane is often the preferred fuel in several situations, such as when natural gas is not available, when propane is more affordable than natural gas, or when a backup fuel source is needed for greater reliability, especially in conjunction with natural gas or diesel [65,66].

Modern gas microturbines are expected to demonstrate a set of advanced features, including reduced emission levels achieved through water or steam injection as well as dry low-emission combustion technologies [67], along with high fuel flexibility enabled by new combustion and fuel systems supported by advanced coatings [68]. Their operation should also ensure improved reliability and availability through extended component lifetimes, intelligent control, and condition monitoring systems, while maintaining higher overall efficiency and enhanced efficiencies of individual components resulting from tighter tolerances and advanced aerodynamic designs. Furthermore, progress is associated with higher firing temperatures, approaching the limits of material effectiveness [69], and the introduction of novel technological solutions such as recuperated cycles (Fig. 9c, [69]), intercooled recuperated cycles [70], integration with high-temperature fuel cells (solid oxide or molten carbonate), power plants equipped with Heat Recovery Steam Generators (HRSG) [71,72], wet cycles [6,70], combined heat and power systems, and photovoltaic integration [73]. At the same time, further developments are expected to reduce costs, increase power density through higher firing temperatures and innovative component designs based on advanced materials such as ceramics [74], and enable more compact turbomachinery with lower component costs resulting from more highly loaded elements.

The advanced cycle is a regenerative Closed Brayton Cycle (CBC) as presented in a paper [73]. The working fluid is a mixture of helium and xenon. The main components of the cycle are: the receiver, which has to collect solar energy, to store it in a phase-change eutectic salt (LiF–CaF_2) and to transfer it to the working fluid, the cooler, which refrigerates the working fluid and ejects the low temperature heat into space via the radiator device; the radial turbomachinery, consisting of the compressor, expander and electrical generator, all assembled on a single rotating shaft, and the recuperator, which recovers the exhaust heat from the expander outlet and transfers it to the compressed air.

Another example is the DynaJet 2.6 portable gas turbine generator, which has a rated output of 2.6 kVA and is shown in Fig. 10.

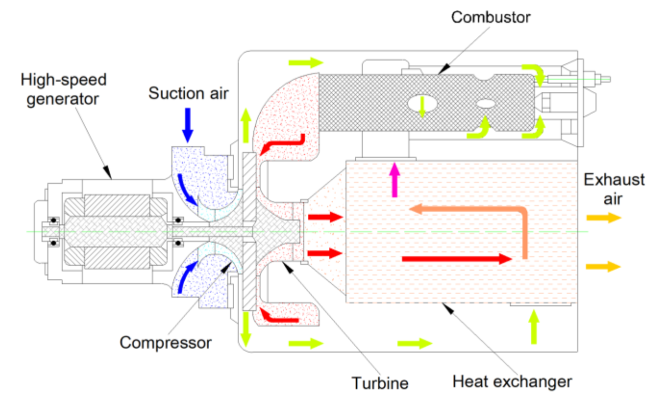

Fig. 10. Schematic diagram of DynaJet 2.6.

The unit is powered by a single-shaft regenerative gas turbine engine. It features a permanent magnet system for the generator, which requires effective cooling to ensure optimal performance at high speeds. The rated rotational speed is 100 000 rpm, and the rated power output is 100 V / 2,6 kVA. The device can operate at a frequency of either 50 Hz or 60 Hz, with the option to switch between these settings. It uses kerosene as fuel, with a consumption rate of less than 4.5 litres per hour at the rated output. The generator operates reliably within a temperature range of 20°C to 50°C. Its dimensions are 825 mm (length), 420 mm (width), and 455 mm (height). Small gas turbines with a power rating of 100 kW or less are attractive not only as distributed power generation systems or for mobile power supply, but also as the core of a combined heat and power system due to the excellent quality of the exhaust gas [75].

Another type of gas turbine is the wave rotor system (Fig. 11). Wave rotors do not use mechanical components such as pistons or blade cascades to compress the fluid. Instead, the pressure increase is achieved by generating compression waves in appropriately designed geometries. It has been proven that, for the same inlet and outlet conditions, wave rotors can significantly enhance performance. The essential feature of wave rotors is an array of channels arranged around the axis of a cylindrical drum. The drum rotates between two end plates, each with several ports or manifolds that control the fluid flow through the channels [76].

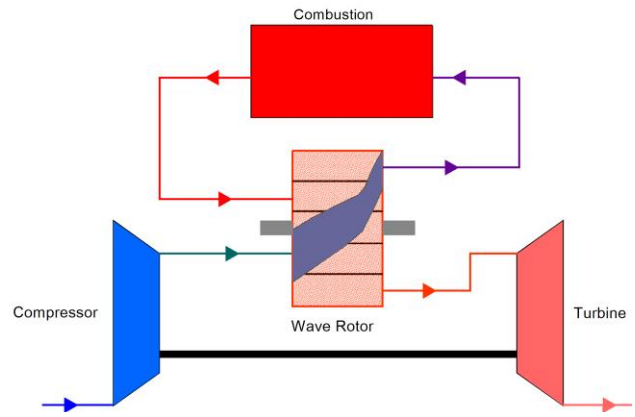

Fig. 11. Schematic diagram of a gas turbine topped by a four-port wave rotor.

The next example is a single-stage axial microturbine. It has been developed with a rotor diameter of 10 mm, see Fig. 12. The turbine is made from stainless steel using die-sinking electro-discharge machining. It has been tested for speeds up to 160 000 rpm and generates a maximum mechanical power of 28 W with an efficiency of 18% [77,78].

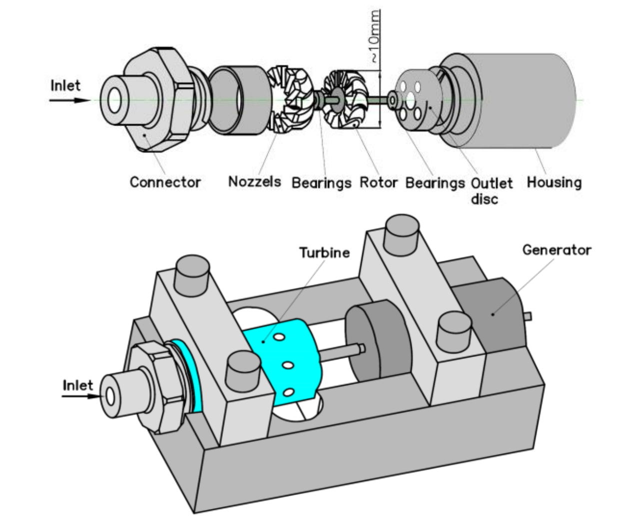

Fig. 12. Single-stage axial microturbine.

In contrast, a groundbreaking solution for a gas microturbine with isothermal expansion can be found in the paper [79] (see Fig. 13). In the proposed solution, the working medium, after isothermal expansion in the nozzles, is transferred to a guide system that provides the correct flow angle to the rotor blades. The rotor of the turbine is shown in Fig. 13a, the compressor in Fig. 13b, and the whole stand is illustrated in Fig. 13c.

a) b) c)

Fig. 13. Isothermal microturbine rotor (a), casing (b) and test rig (c).

The experimental rig consists of the combustion chamber, turbine, compressor, electric generator and regenerator. A large number of tests have been carried out on the operation with various changes and modifications. The test rig is equipped with sensors that measure the temperature and pressure of the working fluid at characteristic points of the unit (at the inlet and outlet of each component), the air flow rate, the rotor speed and the parameters of the electricity generated. The nominal power of the turbine was approximately 5.3 kW, and the rotational speed was 27 000 rpm. It is likely that there will be commercial offers for this type of microturbine set in the near future, as it is the solution with the highest achievable efficiency.

Gas turbines and turbojets are widely used in aviation. Micro jet turbines, on the other hand, have been used in modelling for many years. In these systems, they are small in size and the main parameters are: thrust of several hundred Newtons, temperatures behind the combustion chamber reaching up to 700°C, high revolutions exceeding 100 000 rpm. Table 2 shows examples of micro jet turbines and the operating parameters [80–83].

Microturbines are also used in air-conditioning systems in aircraft – Air Cycle Machine (ACM). ACM systems are the cooling units in the on-board atmosphere control system used in airtight aircraft cabins. Typically, aircraft have two or three ACM

Table 2. Parameters of exemplary airborne microturbines.

No.	Name	Thrust	Temperature, °C	Mass, kg	Diameter, mm	Length, mm	Mass flow, kg/s	Rotational speed, rpm	Compression
1	AMT Olympus	230 N	-	2.475	130	267	0.45	108000	4
2	KH-66	75 N	-	0.93	112	230	0.23	115000	2.2
3	Wren MW54	54 N	-	0.8	87	150	0.18	160000	2.3
4	JF-50 Bee Titanium	63 N	700	0.8	110	170	0.2	180000	2.3
5	JF-160 Rhino	35 lbs	650	1.5	110	300	0.52	116000	-
6	JF-120 SuperEagle	30 lbs	700	1.35	110	300	0.34	128000	2.37
7	Merlin JG-100	27.5 lbs	640	1.25	108	230	0.139	126000	2.37
8	Merlin KJ-66	92 N	590	-	108	230	0.154	128000	1.56
9	Merlin 160G	160 N	550–680	1.45	111	300	0.38	116000	3.2
10	GTM-70	80 N	600	1.2	115	300	-	120000	-
11	FD3 Schreckling	30 N	~700	0.75	-	-	0.16	-	1.5
12	Kamps	50 N	~650	1.14	-	-	0.166	-	2
13	T250P JPX	59 N	~740	1.55	-	-	0.177	-	2.15
14	JF-100 Falcon	22 lbs	650	1.4	98	300	0.27	122000	-
15	JF-50 Bee Tornado	25 N	565	0.4	58	132	0.2	200000	-

units. The cooling process uses air instead of freon in a gas cycle. There is no condensation or evaporation of the working medium in the cycle, the cooled air is used directly to cool the aircraft cabins. The microturbines in these systems run on gas bearings at speeds of 30 000−50 000 rpm [84].

Gas microturbines are increasingly recognised as a key component of modern energy systems, both in industrial applications and in specialised fields such as micro- and nanosatellites. Their design combines compact dimensions with the capability to operate in high-efficiency combined heat and power (CHP) systems as well as in applications requiring high precision and reliability. For space microengines, one of the fundamental design challenges is the modelling of flows in micronozzles and microchannels. The influence of the boundary layer, both laminar and turbulent, on velocity distribution and pressure losses is so significant that dedicated numerical and experimental models are required to design engines capable of delivering thrust in the order of milli-Newtons [85].

Small power turbines can also be found in various means of transport. Rolls-Royce manufactures turbines that have been used to power many small aircraft and helicopters for many years, such as the Bell helicopter. This turbine produces a power output of 533 kW. More than 29 000 units of this turbine have been installed since production began [86].

An older model of the Rolls-Royce 250 turbine was used to power Marine Turbine Technologies (MTT) motorbikes. Installing such a turbine allowed a top speed of around 400 km/h and acceleration from 0 to 320 km/h in around 15 seconds. The turbine produces 286 hp (≈213.4 kW) at 52 000 rpm [87].

Capstone, a company known primarily for its turbines for distributed heat and power generation, was awarded the contract in early April 2008 to manufacture 150 C30 turbines to power buses. The lightweight and robust buses, made mainly of aluminium, will be driven using the energy contained in the batteries; the turbine will only be used to recharge the batteries [88].

Volvo Aero, in turn, also developed a series of microturbines for use in cars, trucks and buses. Between 1988 and 1987, it developed a twin-shaft ceramic microturbine for cars of the KTT MK II/GT110 type with a power output of 115 kW. Later, it produced the new VT40 single-shaft microturbines for cars and the VT100 microturbines for trucks and buses [89].

Jaguar unveiled a prototype of the new Jaguar C-x75 car at the 2010 Paris Motor Show. It is a design that combines gas turbine engine technology with modern electric drive to create a hybrid car. The car has two gas microturbines with 97 hp (≈72.4 kW) each. These are used to drive the generators that charge the battery bank, which drives four electric motors with a total output of 800 hp (≈596.8 KW). The car is able to achieve acceleration in less than 14 s to 300 km/h. The range of this car on a full battery is 90 km, and with turbocharging 900 km can be driven on a full tank. The use of virtually any liquid fuel, gaseous fuel, biofuel, hydrogen, etc. opens a wide door to a new trend in motoring. The Jaguar C-X75 promised to be great, but never went into production [90].

Turbine drive of rotary tools is a relatively recent development and not widely used. In industry, microturbines can be found with powers from 1 to 5 kW, for driving precision tools. They are used as power sources in high-speed grinding spindles, drills, in measuring, control and research apparatus (gyroscopes, mirrors and rotating prisms of laser optical systems, high-speed camera drives, etc.), as expansion turbines in air-conditioning and refrigeration systems and as medical tools (dental and surgical drills). These microturbines operate at relatively low power and high frequencies, so their development has undoubtedly been influenced by the fact that they have mastered the problems of gas bearing to achieve very high frequencies (up to 30 000 Hz and even more). These microturbines are usually powered by compressed air with a pressure of 0.4 to 0.8 MPa and a temperature of about 20°C, drawn from [64].

Medical drills, especially dental drills, were introduced into practice because of the discomfort experienced by patients when preparing hard dental tissue with low-speed drills. The first compressed-air-driven turbine had rolling bearings. Since the mid-1960s, air-bearing drills with a maximum speed of approximately 500 000 rpm have been introduced. These drills are much quieter, and the drill bit is not stimulated to vibrate by the bearing balls. They also do not require oil lubrication and are very durable. Due to these advantages, numerous companies have started to introduce air bearing in the dental drills they manufacture [91,92].

Nowadays, many companies offer, for example, micro turbine tools for precision engraving work based on dental-type turbine cartridges. They offer a low power output of 30–60 W at speeds of up to 400 000 rpm. Thanks to this high speed, the "floating" effect of the cutter tip (torque effect) is minimised [93,94].

Turbine grinders and polishers are another example of the use of microturbines. A turbine grinder offers double the power compared to motorised angle grinders. They are about half the size and weight of motorised tools, offering comparable power. The turbine motor is more efficient than a conventional grinder motor. As a result, it takes less time to do the same amount of work. The overall air consumption is also lower during a specific task. The GTG21 turbine grinder reaches a maximum speed of 12 000 rpm with a power output of 2.1 kW and an air consumption of 30 l/s. The GTG40 turbine grinder, on the other hand, reaches a maximum speed of 8 500 rpm at 4.5 kW and air consumption of 60 l/s. The turbine motor used in these grinders does not need oil in the air for lubrication [95].

Another example of a turbine-driven machine (single-stage axial turbine) with special gas bearings for up to 100 000 rpm and a cutting capacity of up to 100 kW is the TurboTool™ cutting tool [96].

Another way in which microturbines are used are air motors with outputs ranging from 0,1 kW to 35 kW. They have found wide use in industry as a powerful and trouble-free drive motor. They are smoothly controllable over a very wide speed range and provide high starting torque. They can operate at pressures from 2 to 7 bar. The speed of such a motor varies between 2 500 and 7 600 revolutions per minute [97].

A typical microturbine consists of a shaft, on which a generator, a compressor and a turbine are mounted. The turbine shaft rotates at 50 000–100 000 rpm, which corresponds to electrical frequencies ~833–1667 Hz. This power has to be rectified and re-inverted to electrical energy at 50/60 Hz for interfacing with grid power. Rectifiers and inverters are usually very energy efficient but are highly nonlinear, which can negatively affect the system [98–101].

The microturbine control system represents a key problem for stable operation at different working conditions, ensuring a flexible usage of the machine. The experience gained in large-size turbine control systems can also be profitably exploited in the microturbine field, but the time scales of the phenomena are extremely reduced due to the small mechanical inertia of the shafts, which makes microturbines difficult systems to control [102].

Another important development area involves the integration of microturbines with microgrids and hybrid systems. This requires advanced solutions for protection, synchronisation, and control, including adaptive algorithms and diagnostic systems supported by artificial intelligence [103]. In parallel, intensive research is being carried out on the utilisation of alternative fuels, with hydrogen emerging as a particularly promising clean energy carrier for cogeneration and trigeneration systems [104]. These advancements highlight the potential of gas microturbines as a flexible and low-emission technology supporting the transition towards decentralised and sustainable energy systems of the future.

During the last years, we have observed an increasing interest in small nuclear power stations in different countries around the world [105]. It concerns the construction of so-called minireactors (or microreaktors), which are foreseen for energy supplying for houses or military uses. An example is a 200 kW microreactor built in Japan by Japan Atomic Energy Research Institute, which is cooled with liquid sodium. The most interesting thing is that the fuel should be changed every 10 years [106].

The literature analysis of micro gas turbines carried out in this chapter showed that there has been a tremendous development of this technology in the last two decades, and a large variety of proposed designs have emerged. This is due to the very different applications of this type of device. Designers' approaches are focused on improving efficiency, durability, reliability and, of course, low price. The next chapter presents a completely different type of microturbine design solution, namely the adhesion microturbine pioneered by the eminent inventor Nikola Tesla. Devices of this type have been classified in a separate chapter because they can operate as steam microturbines, including those for organic refrigerant vapours, and as gas microturbines.

5. Tesla microturbines

The first adhesion turbine, also known as the Tesla turbine, was designed, built and patented [107] by prominent inventor Nikola Tesla in 1913 (Fig. 14). It was an innovative type of bladeless turbine that operated on a completely different principle to traditional blade turbines.

The operating principle of this type of turbine is based on the phenomena of adhesion and friction, which primarily occur within the boundary layer of fluid between two closely spaced rotating discs. The fluid moves in a spiral pattern through the narrow gap between the discs, travelling from the outer diameter towards the inner diameter. As it flows, the fluid transfers a portion of its kinetic energy to the discs, causing them to rotate. The turbine is powered by one or more inlet nozzles positioned at the outer edge of the discs, directing the working fluid into the gap. The fluid then exits through openings located near the central shaft of the turbine. The distance between the turbine discs is typically very small and is determined by the thickness of the boundary layer.

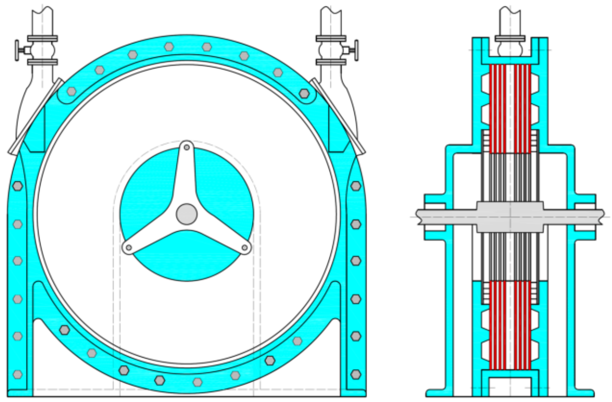

Fig. 14. A view of the Tesla turbine.

Tests conducted by Tesla on real adhesive turbines demonstrated that, as the diameter of the discs increased (and with it the power output, reaching up to 150 kW), structural damage could occur due to material deformation. It is important to note that during the time these experiments were performed, the technology for manufacturing and processing materials capable of withstanding high temperatures and high rotational speeds was limited. Despite the promise of his innovative approach, these material constraints hindered further progress. Tesla's financial situation had deteriorated significantly, and without sufficient resources, he was unable to continue developing and refining the turbine. Ultimately, the combination of material limitations and the absence of financial backing forced Tesla to abandon the project [108,109]. Although he had successfully patented the design and demonstrated its potential in laboratory tests, the adhesive turbine never reached commercial viability in Tesla's lifetime. Nevertheless, his work laid the foundation for future research into bladeless turbines and remains a source of inspiration for engineers and scientists exploring alternative methods of fluid dynamics and energy conversion.

For many years, Tesla’s innovative turbine design was largely overlooked, as the scientific community and industry favoured more conventional technologies like traditional bladed turbines and reciprocating engines. However, by the mid-20th century, there was a renewed interest in alternative turbine designs as researchers sought more efficient and simpler mechanical solutions for energy conversion. It was not until the 1950s that scientists began to revisit Tesla’s ideas, recognising the potential advantages of his bladeless turbine concept, particularly its simplified construction and reduced number of moving parts. One of the pioneers in this research was Armstrong, who in 1952 built his own turbine model. The device was steam-powered and based on the Rankine cycle. Armstrong introduced an innovation by using discs of varying thickness, which increased the rotor's strength and reduced fluid turbulence. Thanks to these modifications, an efficiency of a few per cent was achieved at speeds between 4 000 and 6 000 revolutions per minute [110].

In 1965, Warren Rice, building on Tesla's design, constructed six models that he tested using air as the working fluid. The efficiencies he achieved ranged from 36% to 41%. Using the research results and mathematical analysis, he developed a design relationship between the disc radius and the spacing between them, which allowed the turbines to achieve maximum efficiency at different flow rates. In his conclusions, he noted that Tesla's turbine could be suitable for low-power applications, particularly in situations where low production costs are crucial or where the properties of the working fluid make the use of conventional turbines impractical [111].

In 1966, Beans developed a turbine powered by compressed air. He tested his system for various values of angular velocity, inlet pressure and disc spacing, obtaining efficiencies ranging from 7% to 25% [112]. Although the efficiency values were significantly lower compared to those achieved by Warren Rice, Beans' work provided valuable information on the effects of various operating parameters on turbine performance. By varying the angular velocity, Beans was able to determine the optimum operating speeds for different configurations, highlighting the importance of precise speed control to increase efficiency [113,114].

The reported experimental efficiency of Tesla microturbines in the literature varies considerably, for example:

- 32% efficiency for a turbine with a power output of approximately 3 kW and a rotor speed of 15 000 rpm [115],
- 23% efficiency for a turbine with a power output of approximately 1.5 kW and a rotor speed of 12 000 rpm [116],
- 21% efficiency for a turbine with a power output of approximately 50 W and a rotor speed of 1 000 rpm [33],
- 49% efficiency for a turbine with a power output of approximately 1.56 kW and a rotor speed of 12 000 rpm [112].

For example, the numerical calculations resulted in an efficiency of about 50% obtained for an 11-stage turbine with an output power of about 2 kW at a rotor speed of 18 000 rpm [117].

Tesla's turbine continues to attract significant interest, as evidenced by numerous publications analysing the turbine both theoretically and practically. As demonstrated by the work of Thomazoni et al. [118], the number of publications related to Tesla's turbine has increased significantly in the 21st century. Of these, approximately 36% are analytical studies, 31% are analyses using CFD, 31% are experimental studies, and the remaining 2% are review papers. For example, in the works of Guha and Smiley [119] and Sengupta and Guha [120], similar to Beans, Tesla's turbine was tested by varying selected design parameters. The best configuration solution generated 140 W with an efficiency of about 25%. Modifications to the inlet nozzles were also investigated, which reduced pressure losses and improved efficiency by about 1 percentage point.

In 2015, Krishnan [121], in his qualification work, presented a series of guidelines for the design and construction of Tesla microturbines. The work contains a wealth of valuable data, analyses, and results of experimental studies related to Tesla's turbine and its potential applications. For example, the author determined the minimum radius-to-disc spacing ratio as 20.

Theoretical works employing CFD consider various aspects of designing Tesla-type turbine devices [122]. The efficiency of a Tesla turbine is influenced by both the working fluid parameters (pressure, temperature, inlet velocity) and its kinematics at the inlet and outlet, as well as geometric parameters (distance between rotor discs, diameter, thickness, and number of discs, roughness and micro-topography of their surfaces), rotor rotational speed, and mass flow rate. In the case of mass flow rate, there is a direct influence, namely, the greater the flow, the greater the output power [123]. Similarly, for the initial pressure, analyses have shown that an increase in pressure before the turbine increases efficiency [124]. For example, an increase in pressure by about 1 bar results in an increase in efficiency of about 5% [118].

Regarding the influence of temperature on the efficiency and power of a Tesla turbine, researchers' findings are divided. Publication [125] states that both power and efficiency increase with increasing inlet temperature, while publication [126] demonstrates the ambiguity of the influence of increasing temperature on output power. As in other works, including this one, there are no clear statements regarding the effect of the number and shape of inlet nozzles on turbine efficiency and power, and research in this area is still being developed [127].

In most published cases, the rotational speeds of Tesla turbine rotors are lower than those of bladed turbines [118]. Analyses can be found that define the output power and efficiency of a Tesla turbine as a non-linear function of rotational speed, approximately a second-order polynomial, for a fixed geometry and inlet conditions [128].

The outer diameter of the rotor affects both efficiency and output power. Most studies indicate an increase in turbine output power with an increase in the outer diameter of the rotor. According to some authors, there is an optimal value of the ratio of the outer to inner diameter of the rotor that maximises efficiency [129].

In the case of discs in a Tesla turbine, there is also no consensus among authors. Some argue that there is an optimal number of discs and their thickness that gives the maximum efficiency [130]. Other authors show that the fewer discs, the higher the efficiency [129], while still others argue that efficiency increases with the number of discs [131].

It is quite common to believe that bladed turbines are unrivalled compared to Tesla-type turbines in the range of higher powers, but at very low powers, one can expect a certain advantage of bladeless adhesive turbines [132].

For example, an analytical model incorporating wall roughness through the equivalent sand grain approach was proposed by Rusin et al. [133]. The model modifies dynamic viscosity in the governing equations, allowing the impact of roughness on velocity profiles and turbine efficiency to be assessed. Their results indicate that a surface roughness height of 10^{-5} m can noticeably improve both power output and isentropic efficiency.

In a complementary approach, Pahlavanzadeh et al. [134] introduced a porous layer model (PLM) for directly simulating roughness effects in the gap between rotating disks. This method eliminates the need for equivalent sand grain parameters and was validated against experimental data from minichannel flows. The study demonstrated that increasing surface roughness enhances the interaction between the working fluid and the rotor, thereby influencing overall turbine efficiency.

Similarly, there is no clear consensus on the influence of the number and shape of inlet nozzles on turbine performance. Research in this area is still ongoing [135].

Also worth noting is the growing interest in integrating Tesla turbines with low-temperature heat recovery technologies. A recent study by Teng et al. [136] presents a comprehensive experimental investigation of a Tesla microturbine integrated into an ORC system for low-grade heat recovery (90−130°C). The authors developed a prototype that achieved a maximum output power of 31.76 W and an isentropic efficiency of up to 62.28%, examining the effects of parameters such as heat source temperature, pump speed, and electrical load on system performance. The results highlight the potential of Tesla turbines as efficient and compact solutions for small-scale distributed energy systems and industrial waste heat recovery.

The concept of turbomachinery miniaturisation typically refers to the design of devices with reduced power output, intended to meet the demands of distributed, portable, or microscale systems. These scaled-down machines are used in applications such as portable electronics, IoT sensors, or microenergy systems. Energy micro-generators rely on piezoelectric, electromagnetic, electrostatic, or triboelectric transduction principles, effectively harvesting energy from low-frequency vibrations or human motion. Their power output is inherently limited and tailored to match their miniature form factor [138].

Huynh et al. [137] introduce a pioneering hybrid energy-harvesting system that combines a triboelectric nanogenerator (TENG) and an electromagnetic generator (EMG), both driven by a Tesla turbine. The optimised system achieves peak outputs of 312.5 V / 82 mA (TENG) and 4.2 V / 3.3 mA (EMG), with the hybrid configuration delivering 332 V / 3.5 mA. As demonstrated in the study, the device shows strong potential for use in wearable and low-power portable applications for biomechanical energy harvesting, as illustrated by practical demonstrations such as LED illumination and wireless sensor operation.

The miniaturisation of energy-conversion turbomachinery remains a significant challenge due to the nonlinear scaling of aerodynamic and mechanical phenomena. When reducing the physical size of rotating machines such as Tesla turbines, micro gas turbines, or centrifugal compressors, researchers must address issues including increased viscous effect and reduced flow uniformity. It is well documented that aerodynamic efficiency decreases at low Reynolds numbers due to boundary layer thickening and the dominant influence of viscosity [139].

Based on a literature review and the authors' own experience, a Tesla microturbine was built within a single enclosed hermetic housing (Fig. 15). The concept is based on a novel solution in which the magnets are placed in the rotating disc of the Tesla turbine. The stationary housing, on the other hand, houses the poles where the electric current is induced. The diameter of the disc is 140 mm, the clearance between the moving and stationary disc is approximately 1 mm, and the inlet nozzle is set at an angle of 12° [140,141].

a)

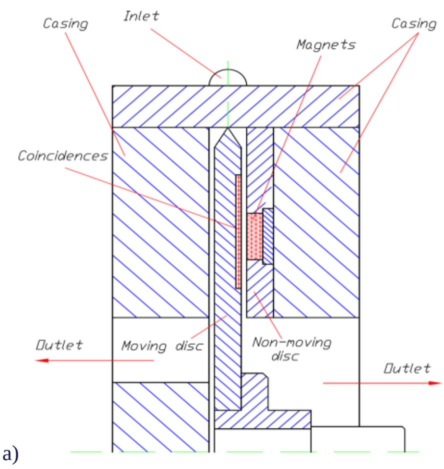

b)

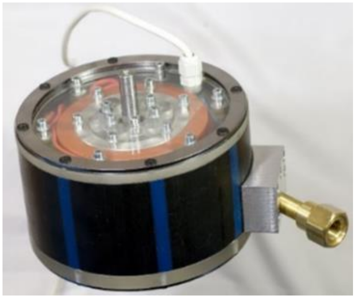

Fig. 15. An overview drawing of the Tesla micro-turbine-generator concept (a); view of the complete disc turbogenerator (b).

The conducted literature analysis has shown that despite the passage of over 100 years since Tesla's invention, work on its development is still ongoing and is certainly not complete. The next supplementary chapter presents examples of steam and gas microturbines made using MEMS technology.

6. Microturbines in MEMS technology

Micro-Electro-Mechanical Systems (MEMS) are miniaturised devices that integrate mechanical and electrical components on a single chip. These systems are fabricated using techniques derived from semiconductor manufacturing, such as photolithography, etching and deposition processes. This technology makes it possible to create devices that typically range in size from a few micrometres to a few millimetres. MEMS devices are extremely small, enabling the creation of compact systems with high functionality. They combine mechanical, electrical, thermal and sometimes optical components into a single system. MEMS devices are designed with nanometre precision and offer exceptional performance in precision applications [142].

Examples of steam microturbines made with MEMS technology are encountered in the literature [143,144]. More on MEMS can be found in publications [145–147], among others. An example of a steam microturbine, implementing the Rankine circuit, made with MEMS technology is presented in Fig. 16.

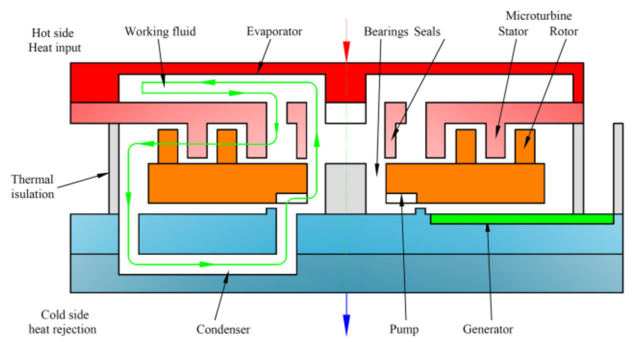

Fig. 16. Cross-section of a steam microturbine power plant on a chip.

The microturbine unit drives a micropump and a power generator and produces electricity with an efficiency of approximately 11%. The basic parameters of the microturbine unit are: steam pressures (inlet/outlet): 0,6/0,18 MPa, steam temperatures (inlet/outlet): 400/316°C, turbine diameters (inlet/outlet): 360/760 mm, blade height: 20−50 mm, steam mass flow rate: 24 mg/s, rotational speed: ~1 000 000 rpm, and the electrical power achieved 5 W.

MEMS technology has been effectively applied to micro gas turbines, resulting in the development of devices with dimensions measured in millimetres, power outputs ranging from 10 to 500 W, and compression ratios between 2:1 and 4:1. These microturbines have been developed alongside semiconductor technology and require exceptional precision during their manufacturing. Their power concentration factor of 33 kWh/kg is more than 20 times higher than that of lithium batteries, which have a density of 1.4 kWh/kg [148]. Microturbines represent a notable application of MEMS technology [149]. One specific example of a gas microturbine built using MEMS technology is the wafer genset, illustrated in Fig. 17.

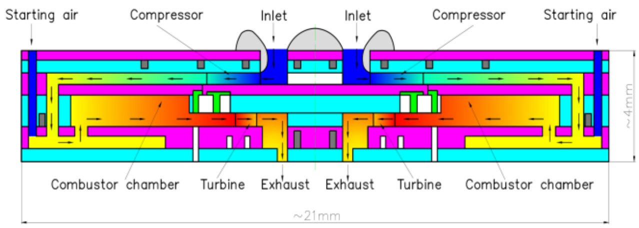

Fig. 17. General view of a wafer microturbine.

This device features a compressor with a diameter of 4 mm and a microturbine with a diameter of 21 mm, while the blade length measures 200 μm. The compressor achieves a tip velocity of 500 meters per second at a rotational speed of 1 million revolutions per minute, with an airflow rate of 0,3 milligrams per second. The blade angle, denoted as α_1, varies between 15° and 20°. The temperature after the combustion chamber reaches 1600 K, and the power density of the combustor chamber is 3 GW/m³, significantly surpassing the typical value of approximately 2 GW/m³ for classical turbines. The radial clearance is around 2 μm, and the cost ranges from 1 000 to 5 000 USD per kilowatt [150]. These parameters underline the remarkable capabilities and efficiency of MEMS-based micro gas turbines.

The economic impact of these devices will be dependent on the performance levels and the manufacturing costs, both of which have yet to be proven. It is certainly possible, however, that MEMS gas turbines may one day be competitive with conventional machines in a cost per installed kilowatt. Even at much higher costs, they will be very useful as compact power sources for portable electronics, equipment, and small vehicles [148]. Figure 18 presents the concept of MEMS gas microturbine engine packaged as a standard military battery. The other advantages of miniaturisation is shortening the time needed for acquiring the information on system behaviour, as well as decreasing the amount of required materials and energy for the manufacturing process.

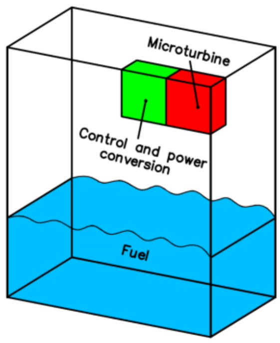

Fig. 18. Concept of MEMS gas microturbine engine packaged as a standard military battery.

Work on this type of device is also being developed, and it seems that in the future it could be used as an autonomous energy source for electronic equipment or small vehicles.

7. Summary

Modern power generation is increasingly focused on moving away from centralised power generation towards distributed systems. Microturbines, whether steam, gas or ORC, are the answer to the growing demand for local, flexible and renewable energy sources. They are a key component of prosumer micro-installations, cogeneration systems and small-scale energy networks (microgrids). Microturbines are extremely diverse in design, power range and application. They can be:

- steam turbines ranging from a dozen watts to hundreds of kilowatts,
- gas-fired microturbines with or without heat recovery,
- turbines in ORC systems to recover waste heat,
- Tesla bladeless turbines, simplified in design,
- MEMS turbines, which function as miniature energy sources, e.g. for portable electronics.

This differentiation allows the solution to be tailored to the specific application, from powering a laptop to recovering heat from a cement plant to driving a turbocharger or micro-generator.

These devices allow energy to be produced close to the point of consumption, minimising transmission losses and increasing supply reliability. Steam and gas microturbine design issues began to develop at the beginning of this century. Technological solutions, although using well-established knowledge of high-power turbines, are at an early stage of development. This requires the integration of knowledge from a number of disciplines, such as:

- thermodynamics (optimisation of thermal cycles),
- fluid mechanics (design of flow systems),
- strength of materials (use of ceramics, aluminium alloys, composites),
- mechatronics and electronics (control systems, energy conversion and storage),
- microengineering (manufacture of MEMS turbines).

The advances concern not only the turbine itself, but entire energy systems including generators, heat exchangers, bearings, gearboxes and cooling systems. Microturbines are part of the green energy transition because they can be:

- powered by biomass, biogas, hydrogen, alcohol, synthesis gas,
- used for waste heat recovery (in ORC, cogeneration, trigeneration),
- coupled to fuel cells or solar collectors,
- used in zero-emission projects (e.g. hydrogen-oxygen combustion).

They are thus part of the drive to decarbonise energy and improve energy efficiency in various sectors of the economy.

Despite tremendous progress, microturbine development still faces a number of technical barriers, including:

- difficulties in miniaturisation and high temperature resistant materials,
- dynamic stability problems at very high speeds (up to 1 million rpm in MEMS),
- challenges in lubrication and cooling (e.g. oil-free bearings),
- complications in designing very efficient, small heat exchangers,
- the need for precision control systems and power electronics (e.g. for high-frequency generators).

Key research directions in the coming years will be:

- increasing efficiency to > 40%,
- lowering the investment cost below 500 USD/kW,
- development of multi-fuel and zero-emission drives,
- integrated hybrid systems (e.g. microturbine + photovoltaics (PV) + energy storage),
- implementation of advanced materials (ceramics, superalloys).

Microturbines are increasingly used in means of transport (cars, motorbikes, buses, drones, aircraft) as:

- power sources,
- energy recovery systems (e.g. turbochargers),
- direct drives (in hybrids or research models).

In industry, they are used for:

- powering high-speed instruments (e.g. dental turbines),
- powering mobile diagnostic equipment,
- air conditioning and refrigeration (e.g. in aviation).

This shows that microturbines not only produce energy but also increase the efficiency of other technical systems.

The review of existing steam and gas microturbine designs carried out in this article does not provide clear answers as to what direction their development will take. According to the authors, the observed trends in the development of these devices allow the conclusion that they will move towards the construction of more efficient, reliable, and sustainable microturbines, both steam and gas. Analyses have also shown that there is now also a very strong emphasis on emissions, so the development of these devices will also move towards the use of low- or zero-emission fuels, such as hydrogen.

References

[1] Aquaro, D., & Pieve, M. (2007). High temperature heat exchangers for power plants: Performance of advanced metallic recuperators. *Applied Thermal Engineering*, 27(2), 389−400. doi: 10.1016/j.applthermaleng.2006.07.030

[2] Soares, C. (2007). *Microturbines* (1st ed.). Butterworth- Heinemann; Oxford, United Kingdom.

[3] Kolanowski, B.F. (2004). *Guide to Microturbines* (1st ed.). Marcel Dekker, New York, United States.

[4] Epstein, A.H., Senturia, S.D., Al-Midani, O., Anathasuresh, G., Ayon, A., Breuer, K., Chen, K-S., Ehrich, F.E., Esteve, E., Frechette, L., Gauba, G., Ghodssi, R., Groshenry, C., Jacobson, S., Kerrebrock, J.L., Lang, J.H., Lin, C-C., London, A., Lopata, J., Mehra, A., Mur, M.J.O., Nagle, S., Orr, D.J., Piekos, E., Schmidt, M.A., Shirley, G., Spearing, S.M., Tan, C.S., Tzeng, Y-S., & Waitz, I.A. (1997). *Micro-Heat Engines, Gas Turbines, and Rocket Engines - the MIT Microengine Project*. American Institute of Aeronautics and Astronautics Inc., AIAA97-1773.

[5] Epstein, A.H., Senturia, S.D., Anathasuresh, G., Ayon, A., Breuer, K., Chen, K-S., Ehrich, F.E., Gauba, G., Ghodssi, R., Groshenry, C., Jacobson, S., Lang, J.H., Lin, C-C., Mehra, A., Mur, M.J.O., Nagle, S., Orr, D.J., Piekos, E., Schmidt, M.A., Shirley, G., Spearing, S.M., Tan, C.S., Tzeng, Y-S., & Waitz, I.A. (1997). Power MEMS and Microengines. *IEEE Transducers'97 Conference*, 19 June, Chicago, United States.

[6] Kosowski, K. (2001). *Steam and Gas Turbines with the Examples of Alstom Technology*. Alstom: Saint-Quen, France.

[7] Beith, R. (2011). *Small and micro combined heat and power CHP systems*. Woodhead Publishing Limited, Sawston, Cambridge, United Kingdom.

[8] Gailfuß, M. (2003). Private meets Public—Small Scale CHP; Technological Developments, *Workshop BHKW-Infozentrum Rastatt*, 9 Sept., Berlin, Germany.

[9] Pujari, V., Vartabedian, A., Collins, B., & Garrett, J. (2005). Optimization of High Temperature Silicon Nitride for Microturbine Applications. *Proceedings of the 29 th International Conference on Advanced Ceramics and Composites*, January 23−28, Cocoa Beach, Florida, United States.

[10] Breuer, K.S. (2000). *MEMS Sensors for Aerodynamic Measurements - the Good, the Bad and the Ugly*. American Institute of Aeronautics and Astronautics Inc., AIAA00-0251.

[11] Bonnie, S. (2004). Overview of Microturbines Powered by Steam. *Colorado Wind and Distributed Energy Conference Bio-Energy Corporation*, 14 May, Colorado, United States.

[12] Colombo, L.P.M., Armanasco, F., & Perego, O. (2007). Experimentation on a Cogenerative System Based on a Microturbine. *Applied Thermal Engineering*, 27, 705−711. doi: 10.1016/j.applthermaleng.2006.10.005

[13] Kiciński, J., &·Żywica, G. (2014). *Steam Microturbines in Distributed Cogeneration*. Springer Cham Heidelberg New York Dordrecht London, Springer International Publishing Switzerland.

[14] Valencia, H.D. (2005). *Vertical Steam Turbine Generators: Opening a New Market for Energy Recovery Industrial Water Chillers*. Carrier Corporation, Syracuse, New York.

[15] Riggi, A.L. (2014). Mississippi Cooling, Heating, and Power (micro-CHP) and Bio-fuel Center. *Technical report*, United States Department of Energy. doi: 10.2172/1178540

[16] Efimov, N.N., Papin, V.V., & Bezuglov R.V. (2016). Micro Energy Complex Based on Wet-SteamTurbine. *Procedia Engineering*, 150, 324–329. doi: 10.1016/j.proeng.2016.07.022

[17] Sarnacki, W.P., Kimball, R., & Fleck, B. (2007). Development of a Combined Cycle Gas Turbine/Steam plant for Training Marine and Power Engineers. *Proceedings of ASME Turbo Expo 2007 Power and Land, Sea and Air*, 14−17 May, Montreal, Canada.

[18] *Electronic document, home page*. http://www.nestco1.com/ index.htm [accessed 27 Dec. 2011].

[19] Post, J. (2012). *Microturbine System and Method for Generating Electricity*, European Patent, EP 2 203 629 B1.

[20] Peng, N., Wang, E., Wang, W., Lu, J., & Li, M. (2024). Aerodynamic analysis of a 1.5 kW two-stage counter-rotating partial-admission impulse turbine for small-scale power system with a high expansion pressure ratio. *Case Studies in Thermal Engineering*, 53, 103824. doi: 10.1016/j.csite.2023.103824

[21] Paulides, J.J.H., Post, E., Post, J, Encica, L., & Lomonova, E.A. (2015). Green Turbine: A High Speed Double Turbine for Sustainable Energy Harvesting from Waste Heat. *10th International Conference on Ecological Vehicles and Renewable Energies (EVER)*, 31 March – 2 April, Monte-Carlo, Monaco. doi: 10.1109/EVER.2015.7112926

[22] Efimov, N.N., Parshukov, V.I., Oshchepkov, A.S., Ryzhkov, A.V., Rusakevich, I.V., & Blokhin E.E. (2023). Steam plant based on high-speed active microturbine with valve-inductor generator as part of power engineering complex for processing of CURRENT and power plant for hydrogen production, *International Journal of Hydrogen Energy*, 48, 18557–18566. doi: 10.1016/j.ijhydene.2023.01.368.

[23] Mirzaei, M.R., Kasaeian, A., Motlagh, M.S., & Fereidoni, S. (2024). Thermo-economic analysis of an integrated combined heating, cooling, and power unit with dish collector and organic Rankine cycle. *Energy*, 296, 131089. doi: 10.1016/j.energy.2024.131089

[24] Kalair, A.R., Seyedmahmoudian, M., Stojcevski, A., Mekhilef, S., Abas, N., & Koh, K. (2023). Thermal comfort analysis of a trombe wall integrated multi-energy nanogrid building. *Journal of Building Engineering*, 78, 107623. doi: 10.1016/j.jobe.2023.107623

[25] Cano, A., Arévalo, P., Benavides, D., & Jurado, F. (2021). Sustainable tramway, techno-economic analysis and environmental effects in an urban public transport. A comparative study. *Sustainable Energy, Grids and Networks*, 26, 100462. doi: 10.1016/j.segan.2021.100462

[26] *Creating Educational Laboratory Equipment For Tomorrow's Engineer „MiniLab Gas Turbine Power System"*, http://www.turbinetechnologies.com/steam.html [accessed 26 Jan. 2008].

[27] Tartière, T., & Astolfi, M.A. (2017). World Overview of the Organic Rankine Cycle Market. *Energy Procedia*, 129, 2–9. doi: 10.1016/j.egypro.2017.09.159

[28] Quoilin, S., Broek, M., Declaye, S., Dewallef, P., & Lemort, V. (2013). Techno-economic survey of Organic Rankine Cycle (ORC) systems. *Renewable and Sustainable Energy Reviews*, 22, 168–186. doi: 10.1016/j.rser.2013.01.028

[29] Mikielewicz, D., & Mikielewicz, J. (2008). Cogenerative micro power plants − A new direction for development of power engineering? *Archives of Thermodynamics*, 29, 109–132.

[30] Mikielewicz, J., & Mikielewicz, D. (2009). Comparative study of selected fluids for use in supercritical Organic Rankine Cycles. *Archives of Thermodynamics*, 30, 3–15.

[31] Simader, G.R., Krawinkler, R., & Trnka, G. (2006). Micro CHP systems: state-of-the-art. *Final Report, Deliverable 8 (D8) of Green Lodges Project (EIE/04/252/S07.38608)*, Austrian Energy Agency, Vienna, Austria.

[32] Quoilin, S., Declaye, S., Tchanche, B.F., & Lemort, V. (2011). Thermo-economic optimization of waste heat recovery Organic Rankine Cycles. *Applied Thermal Engineering*, 31, 2885−2893. doi: 10.1016/j.applthermaleng.2011.05.014

[33] Lecompte, S., Huisseune, H., Van den Broek, M., Vanslambrouck, B., & DePaepe, M. (2015). Review of organic Rankine cycle (ORC) architectures for waste heat recovery. *Renewable and Sustainable Energy Reviews*, 47, 448–461, doi: 10.1016/j.rser.2015.03.089

[34] Zhao, Y., Liu, G., Li, L., Yang, Q., Tang, B., & Liu, Y. (2019). Expansion devices for organic Rankine cycle (ORC) using in low temperature heat recovery: A review. *Energy Conversion and Management*, 199, 111944. doi: 10.1016/j.enconman.2019.111944

[35] Kermani, M., Wallerand, A.S., Kantor, I.D., & Maréchal, F. (2018). Generic superstructure synthesis of organic Rankine cycles for waste heat recovery in industrial processes. *Applied Energy*, 212, 1203–1225. doi: 10.1016/j.apenergy.2017.12.094

[36] Da Silva, J.A.M., Seifert, V., de Morais, V.O.B., Tsolakis, A., Herreros, J., & Torres, E. (2018). Exergy evaluation and ORC use as an alternative for efficiency improvement in a CI-engine power plant. *Sustainable Energy Technologies and Assessments*, 30, 216–223. doi: 10.1016/j.seta.2018.10.007.

[37] Li, T., Meng, N., Liu, J., Zhu, J., & Kong, X. (2019). Thermodynamic and economic evaluation of the organic Rankine cycle(ORC) and two-stage series organic Rankine cycle (TSORC) for flue gas heat recovery. *Energy Conversion and Management*, 183, 816–829. doi: 10.1016/j.enconman.2018.12.094

[38] Altun, A.F., & Kilic, M. (2020). Thermodynamic performance evaluation of a geothermal ORC power plant. *Renewable Energy*, 148, 261-274. doi: 10.1016/j.renene.2019.12.034

[39] Tartiere, T., & Astolfi, M. (2017). A World Overview of the Organic Rankine Cycle Market. *Energy Procedia*, 129, 2−9. doi: 10.1016/j.egypro.2017.09.159

[40] Piwowarski, M. (2013). Design analysis of ORC microturbines making use of thermal energy of oceans. *Polish Maritime Research*, 20(2), 48−60. doi: 10.2478/pomr-2013-0016

[41] Quoilin, S., & Lemort, V. (2009). Technological and Economical Survey of Organic Rankine Cycle Systems. *Proceedings of the 5-th European Conference Economics and Management of Energy in Industry*, 14−17 April, Vilamoura, Portugal.

[42] Kosowski, K., Piwowarski, M., Stepien, R., & Włodarski, W. (2018). Design and investigations of the ethanol microturbine. *Archives of Thermodynamic*, 39, 41–54. doi: 10.1515/aoter-2018-0011

[43] Landelle, A., Tauveron, N., Haberschill, P., Revellin, R., & Colasson, S. (2017). Organic Rankine cycle design and performance comparison based on experimental database. *Applied Energy*, 204, 1172–1187.

[44] Colonna, P., Nannan, N.R., Guardone, A., & Lemmon E.W. (2006). Multiparameter equations of state for selected siloxanes. *Fluid Phase Equilibria*, 244(2), 193–211. doi: 10.1016/j.fluid.2006.04.015

[45] Tchanche, B.F., Lambrinos, Gr.. Frangoudakis, A., & Papadakis, G. (2011). Low-grade heat conversion into power using organic Rankine cycles – A review of various applications. *Renewable*

and Sustainable Energy Reviews, 15(8), 3963–3979. doi: 10.1016/j.rser.2011.07.024

[46] Stępniak, D., & Piwowarski, M. (2014). Analyzing selection of low-temperature medium for cogeneration micro power plant. *Polish Journal of Environmental Studies*, 23, 1417–1421.

[47] Kosowski, K., & Piwowarski, M. (2020). Subcritical Thermodynamic Cycles with Organic Medium and Isothermal Expansion. *Energies*, 13, 4340. doi: 10.3390/en13174340

[48] Vescovo, R., & Spagnoli, E. (2017). High Temperature ORC Systems. *Energy Procedia*, 129, 82−89. doi: 10.1016/j.egypro.2017.09.160

[49] Piwowarski, M., & Kosowski, K. (2020). Advanced Turbine Cycles with Organic Media. *Energies*, 13, 1327. doi: 10.3390/en13061327

[50] Braimakis, K., & Karellas, S. (2018). Energetic optimization of regenerative Organic Rankine Cycle (ORC) configurations. *Energy Conversion and Management*, 159, 353–370. doi: 10.1016/j.enconman.2017.12.093

[51] Abam, F.I., Ekwe, E.B., Effiom, S.O., Ndukwu, M.C., Briggs, T.A., & Kadurumba, C.H. (2018). Optimum exergetic performance parameters and thermo-sustainability indicators of low-temperature modified organic Rankine cycles (ORCs). *Sustainable Energy Technologies and Assessments*, 30, 91–104. doi: 10.1016/j.seta.2018.09.001

[52] Imran, M., Park, B.S., Kim, H.J., Lee, D.H., Usman, M., & Heo, M. (2014). Thermo-economic optimization of Regenerative Organic Rankine Cycle for waste heat recovery applications. *Energy Conversion and Management*, 87, 107−118. doi: 10.1016/j.enconman.2014.06.091

[53] Li, T., Zhu, J., Hu, K., Kang, Z., & Zhang, W. (2014). Implementation of PDORC (parallel double-evaporator organic Rankine cycle) to enhance power output in oilfield. *Energy*, 68, 680−687. doi: 10.1016/j.energy.2014.03.007

[54] Vetter, Ch., Wiemer, H.-J., & Kuhn, D. (2013). Comparison of sub- and supercritical Organic Rankine Cycles for power generation from low-temperature/low-enthalpy geothermal wells, considering specific net power output and efficiency. *Applied Thermal Engineering*, 51, 871−879. doi: 10.1016/j.applthermaleng.2012.10.042

[55] Xia, X.X., Qi W.Z., Hua, H.Y., & Jun, Z.N. (2018). A novel comprehensive evaluation methodology of organic Rankine cycle for parameters design and working fluid selection. *Applied Thermal Engineering*, 143, 283–292. doi: 10.1016/j.applthermaleng.2018.07.061

[56] Zaniewski, D., Klimaszewski, P., Klonowicz, P., Lampart, P., Witanowski, Ł., Jędrzejewski, Ł., Suchocki, T., & Antczak, Ł. (2021). Performance of the honeycomb type sealings in organic vapour microturbines. *Energy*, 226, 120242. doi: 10.1016/j.energy.2021.120242

[57] Kaczmarczyk, T.Z., & Żywica, G. (2024). Experimental study of the effect of load and rotational speed on the electrical power of a high-speed ORC microturbogenerator. *Applied Thermal Engineering*, 238, 122012. doi: 10.1016/j.applthermaleng.2023.122012

[58] Mieloszyk, M., Majewska, K., Żywica, G., Kaczmarczyk, T.Z., Jurek, M., & Ostachowicz, W. (2020). Fibre Bragg grating sensors as a measurement tool for an organic Rankine cycle microturbogenerator. *Measurement*, 157, 107666. doi: 10.1016/j.measurement.2020.107666

[59] Zuo, Q., Liu, P., Meng, W., Zeng, X., Li, H., Wang, H., Tian, H., & Shu, G. (2025). Bayesian optimized LSTM-based sensor fault diagnosis of organic Rankine cycle system. *Energy and AI*, 21, 100519. doi: 10.1016/j.egyai.2025.100519

[60] Piwowarski, M., Kosowski, K., & Richert, M. (2023). Organic Supercritical Thermodynamic Cycles with Isothermal Turbine. *Energies*, 16, 4745. doi: 10.3390/en16124745

[61] Cohen, H., Rogers, G.F.C., & Saravanamuttoo, H.I.H. (1987). *Gas Turbine Theory* (3 rd ed.), Longman Scientific & Technical.

[62] Kesseli, J., Sullivan, S., Swarden, M., Duffy, S.F., Baker, E.H., Ferber, M., & Jounkouski, J. (2003). Advancements in the IR PowerWorks Employing a Ceramic Turbine Rotor, *International Gas Turbine Institute, IGTI Microturbine Session*, June 16, 2003.

[63] Konecna, E., Masa, V., Miklas, V., Slovak, R., Jordening, A., & Blaha, V. (2023). Gas microturbine as a main source of energy for industrial laundry – feasibility study, *Energy*, 267, 126630. doi: 10.1016/j.energy.2023.126630

[64] Kazimierski, Z., & Krysiński, J. (1981). *Gas bearing and microturbine drives*. WNT Warszawa (in Polish).

[65] Boyce, M.P. *Gas Turbine Engineering Handbook* (2nd ed.), Gulf Professional Publishing, An Imprint of Butterworth-Heinemann, Boston, Oxford, Auckland, Johannesburg, Melbourne, New Delhi.

[66] Logan, E. Jr., & Ro, R. (2003). *Handbook of Turbomachinery* 2nd ed.), Arizona State University, Marcel Dekker Inc. New York, Basel.

[67] McDonald, C.F. (2003). Recuperator considerations for future higher efficiency microturbines. *Applied Thermal Engineering*, 23(12), 1463–1487. doi: 10.1016/S1359-4311(03)00083-8.

[68] *Advanced Catalytic Reactors and Systems for the Energy Sector. Clean Power Solutions for the 21st Century*. (2004). http://www.precision-combustion.com/products.html, Precision Combustion, INC. Company Capabilities [accessed 4 Nov. 2024].

[69] Haught, D. (2004). Final ATS Annual Program Review Meeting. *Clean Energy for 21 st Century*, December 4− 6, Alexandria, VA.

[70] Horlock, J.H. (2003). *Advanced Gas Turbine Cycles* (1st ed.). An imprint of Elsevier Science, Amsterdam, Boston, Heidelberg, London, New York, Oxford, Paris, San Dego, San Francisco, Singapore, Sydney, Tokyo.

[71] Brown, M. (2004). An Introduction to Gas Turbines & Microturbines for DE Applications. *World Energy Technologies Summit*, 10–11 February.

[72] Spentzas, S., Chimack, M., & Worek, W. (2006). Optimization of a Cogeneration System in the Automotive Industry. *SAE 2006 World Congress & Exhibition*. *SAE Technical Paper 2006-01-0831.* doi: 10.4271/2006-01-0831

[73] *Microturbine Systems Big Energy Savings in a Small Package PowerWorks*. (2005). Ingersoll-Rand Energy Systems.

[74] Kang, S., Johnston, J.P., Arima, T., Matsunaga, M., Tsuru, H., & Printz, F.B. (2004). Microscale Radial-Flow Compressor Impeller Made of Silicon Nitride: Manufacturing and Performance. *Transactions of the ASME, Journal of Engineering for Gas Turbines and Power*, 126, 358−365. doi: 10.1115/1.1739246

[75] Kumakura, H., Maekawa, H., & Murakami, K. (2004). Development of Portable Gas Turbine Generator "Dynajet 2.6". *IHI Engineering Review*, 37(3), 113−114.

[76] Akbari, P., Nalim, R., & Müller, N. (2006). Performance Enhancement of Microturbine Engines Topped with Wave Rotors. *Transactions of the ASME, Journal of Engineering for Gas Turbines and Power*, 128, 190−202. doi: 10.1115/1.1924484

[77] Peirs, J., Reynaerts, D., & Verplaetsen, F. (2003) Development of an axial microturbine for a portable gas turbine generator. *Journal of Micromechanics and Microengineering*, 13, S190. doi: 10.1088/0960-1317/13/4/328

[78] Peirs, J., Reynaerts, D., & Verplaetsen, F. (2004). A microturbine for electric power generation. *Sensors and Actuators A: Physical*, 113(1), 86−93. doi: 10.1016/j.sna.2004.01.003

[79] Kosowski, K., Piwowarski, M., Richert, M., Stępień, R., & Włodarski, W. (2024). Isothermal turbines New challenges. Numerical and experimental investigations into isothermal expansion in turbine power plants. *Energy Conversion and Manage*ment, 315, 118772. doi: 10.1016/j.enconman.2024.118772
[80] Kamps, T. (2005). *Model Jet Engines* (3rd ed.). Traplet Publication Ltd., North Las Vegas, NV, U.S.A.
[81] Rowbotham, R. (2005). *Merlin 160 G Instruction Manual-Version 1.1.2005*. Cami del Pollastre, 108358, Arenys de Munt, Barcelona, Spain.
[82] http://www.jetmodel.webpark. pl/silniki.html [accessed 27 Dec. 2011] (in Polish).
[83] http://www.artesjet.com/products.htm [accessed 27 Dec. 2011].
[84] http://www.mt-online.com/component/content/article/67-may/538-balance-and-vibration-test-solutions-for-air-cycle-machines.html [accessed 27 Dec. 2011].
[85] Boryaev, A.A. (2021). Boundary layer calculation in gas flows in micronozzles. *International Journal of Non-Linear Mechanics*, 137, 103831. doi: 10.1016/j.ijnonlinmec.2021.103831
[86] http://www.fh1100.com/250.html [accessed 28 Dec. 2011].
[87] http://www.marineturbine.com/motorcycles.asp [accessed 28 Dec. 2011].
[88] http://www.capstoneturbine.com [accessed 28 Dec. 2011].
[89] Gabrielsson, R. (2005). Microturbines Volvo Aero Corporation. *Personal communication*, 117.
[90] https://moto.pl/MotoPL/7,88389,27944219,jaguar-c-x75-z-spectre-nigdy-nie-wszedl-do-produkcji-jednak.html [accessed 4 Nov. 2024] (in Polish).
[91] http://stoma.abc24.pl/default.asp?kat=12968&pro=63806 [accessed 28 Dec. 2011].
[92] http://www.elmedes.pl/index.php?m=2&subview=82&id=46, [accessed 28 Dec. 2011].
[93] http://atmo.com.pl/portal/product/450/szlifierka-bezolejowa-wysokoobrotowa-biax-85-tys [accessed 28 Dec. 2011] (in Polish).
[94] http://atmo.hrba.flexopartner.net/portal/product/ 451/szlifierka-bezolejowa-wysokoobrotowa-biax-100-tys [accessed 28 Dec. 2011] (in Polish).
[95] http://www.narzedzia-pneumatyka.info/pl/szlifierki/ [accessed 28 Dec. 2011] (in Polish).
[96] http://pergatory.mit.edu/perg/awards/TURBOTOO.html [accessed 29 Dec. 2011].
[97] http://www.pressura.com/demag/motoren/katalog/silniki4.pdf [accessed 29 Dec. 2011] (in Polish).
[98] Kirawanich, P., & O'Connell, R.M. (2003). Potential Harmonic Impact of Microturbines on a Commercial Power Distribution System. *Institute of Electrical and Electronics Engineers (IEEE)*, 1118−1123.
[99] *Environmental Technology Verification Report*. *Ingersoll-Rand Energy Systems IR PowerWorksTM 70 kW Microturbine System*. (2003). SRI/USEPA-GHG-VR-21. Greenhouse Gas Technology Center, Southern Research Institute, U.S. Environmental Protection Agency, New York State Energy Research and Development Authority, USA.
[100] Staunton, R.H., & Ozpineci, B. (2003). *Microturbine Power Conversion Technology Review*. Report ORNL/TM-2003/74. April 8, OAK Ridge National Laboratory, Oak Ridge, Tennessee 37831, USA.
[101] Walsh, P.P., & Fletcher, P. (2004). Gas Turbine Performance (2nd ed.). Blackwell Science Ltd, Oxford, UK. doi: 10.1002/9780470774533
[102] Traverso, A., Calzolari, F., & Massardo, A. (2005). Transient Analysis of and Control System for Advanced Cycles Based on Micro Gas Turbine Technology. *Journal of Engineering for Gas Turbines and Power*, 127, 340−347. doi: 10.1115/1.1839918
[103] Kumar, K., Kumar, P., & Kar, S. (2024). A review of microgrid protection for addressing challenges and solutions. *Renewable Energy Focus*, 49, 100572. doi: 10.1016/j.ref.2024.100572
[104] Kamran, M., & Turzyński, M. (2024). Exploring hydrogen energy systems: A comprehensive review of technologies, applications, prevailing trends, and associated challenges. *Journal of Energy Storage*, 96, 112601. doi: 10.1016/j.est.2024.112601
[105] Schock, R.N., Brown, N.W., & Smith, C.F. (2001). Nuclear Power, Small Nuclear Technology, and the Role of Technical Innovation. *Conference: New Energy Technologies: A Policy Framework for Micro-Nuclear Technology*, 9 Mar., Houston, USA.
[106] Jezierski, G. (2005). Increased interest in small nuclear power plants, *Energia Gigawat*, 12 (in Polish).
[107] Tesla, N. (1913). *Turbine*, Patent No. 1,061,206. United States Patent Office, N.Y., May 6.
[108] Cairnes, W.M.J. (2001). *The Tesla Disc Turbine*. Camden Miniature Steam Services, USA.
[109] Ladino, A.F.R. (2004). *Numerical simulation of the flow field in a friction-type turbine (Tesla turbine)*. Diploma Thesis, Vienna University of Technology, Austria.
[110] Armstrong, J.H. (1952). *An Investigation of the Performance of a Modified Tesla Turbine*. A Thesis Presented to the Faculty of the Division of Graduate Studies, Georgia Institute of Technology, USA.
[111] Rice, W. (1965). An Analytical and Experimental Investigation of Multiple-Disk Turbines. *Journal of Engineering for Gas Turbines and Power, Transaction of the ASME*, 87(1), 29−36, doi: 10.1115/1.3678134
[112] Davydov, A.B., & Sherstyuk, A.N. (1980). Experimental Research on a Disc Microturbine. *Russian Engineering Journal*, 60(8), 19–22.
[113] Beans, W.E. (1966). Investigation Into the Performance Characteristics of a Friction Turbine, *Journal of Spacecraft and Rockets*, 3(1), 131−134. doi: 10.2514/3.28398
[114] North, R.C. (1969). *An Investigation of the Tesla Turbine*. Thesis, University of Maryland.
[115] Gruber, E.L. (1960). *An Investigation of a Turbine with a Multiple Disc Rotor*. Thesis, Arizona State University, Tempe, Arizona, 1960.
[116] Rice, W. (1991). Tesla Turbomachinery. *Conference Proceedings of the IV International Tesla Symposium*, Serbian Academy of Sciences and Arts, 22−25 Sept. Belgrade, Yugoslavia.
[117] Schmidt, D.D. (2002). Final Report Biomass Boundary Layer Turbine Power. *Energy Innovations Small Grant*, EISG Final Report, Appendix A FAR 00-06.
[118] Thomazoni, A.L.R., Ermel, C., Schneider, P.S., Vieira, L.W., Hunt, J.D., Ferreira, S.B., Rech, Ch., & Gouvea, V.S. (2022). Influence of operational parameters on the performance of Tesla turbines: Experimental investigation of a small-scale turbine. *Energy*, 261, 125159. doi: 10.1016/j.energy.2022.125159
[119] Guha, A., & Smiley, B. (2010). Experiment and analysis for an improved design of the inlet and nozzle in Tesla disc turbines. *Proceedings of the Institution of Mechanical Engineers, Part A: Journal of Power and Energy*, 224, 261–277. doi: 10.1243/09576509 JPE818
[120] Sengupta, S., & Guha, A. (2012). A theory of Tesla disc turbines. *Proceedings of the Institution of Mechanical Engineers, Part A: Journal of Power and Energy*, 226(5), 650–663. doi: 10.1177/0957650912446402
[121] Krishnan, V.(2015). *Design and Fabrication of cm-scale Tesla Turbines*. PhD dissertation, University of California, June 1, Berkeley, USA.

[122] Alonso, D.H., & Silva, E.C.N. (2022). Topology optimization applied to the design of Tesla-type turbine devices. *Applied Mathematical Modelling*, 103, 764–791. doi: 10.1016/j.apm.2021.11.007

[123] Li, R., Wang, H., Yao, E., Li, M., & Nan, W. (2017). Experimental study on bladeless turbine using incompressible working medium. *Advances in Mechanical Engineering*, 9(1). doi: 10.1177/1687814016686935.

[124] Qi, W., Deng, Q., Feng, Z., & Yuan, Q. (2016). Influence of disc spacing distance on the aerodynamic performance and flow field of Tesla turbines. *Conference: ASME Turbo Expo 2016: Turbomachinery Technical Conference and Exposition*, June 13−17, Seoul, South Korea. doi: 10.1115/GT2016-57971

[125] Manfrida, G., Pacini, L., & Talluri, L. (2018). An upgraded Tesla turbine concept for ORC applications. *Energy*, 158, 33–40. doi: 10.1016/j. energy.2018.05.181

[126] Deng, Q., Qi, W., & Feng, Z. (2013). Improvement of a theoretical analysis method for tesla turbines. *ASME Turbo Expo 2013: Turbine Technical Conference and Exposition*, June 3−7, San Antonio, Texas, USA. doi: 10.1115/gt2013-95425

[127] Kamran, M.A., & Manzoor, S. (2020). Effect of nozzle angle, turbine inlets and mass flow rate on the performance of a bladeless turbine. *Proceeding of the Institution of Mechanical Engineering, Part A: Journal of Power and Energy*, 234(8), 1101–1107. doi: 10.1177/0957650919893539

[128] Klingl, S., Lecheler, S., & Pfitzner, M. (2019). Experimental, numerical and theoretical investigations of Tesla turbines. *E3S Web of Conferences*, 113, 03003doi: 10.1051/e3 sconf/201911303003

[129] Talluri, L., Fiaschi, D., Neri, G., & Ciappi, L. (2018). Design and optimization of a Tesla turbine for ORC applications. *Applied Energy*, 226, 300−319. doi: 10.1016/j. apenergy.2018.05.057

[130] Pfenniger, A., Vogel, R., Koch, V.M., & Jonsson, M. (2014). Performance analysis of a miniature turbine generator for intracorporeal energy harvesting. *Artificial Organs*, 38(5), E68−E81. doi: 10.1111/aor.12279

[131] Shaw, D., Liu, F.T., & Yu, J.J. (2013). Experiment of a tesla engine for wind energy capture. *Applied Mechanics and Materials*, 284–287, 1051–1056. doi: 10.4028/www.scientific.net/AMM.284-287.1051

[132] Lampart, P., Kosowski, K., Piwowarski, M., & Jędrzejewski, Ł. (2009). Design analysis of Tesla microturbine operating on a low-boiling medium. *Polish Maritime Research*, S1, 28−33. doi: 10.2478/v10012-008-0041-5

[133] Rusin, K., Wróblewski, W., Malekshah, E.H., Pahlavanzadeh, M., & Rulik, S. (2024). Extended analytical model of tesla turbine with advanced modelling of velocity profile in minichannel between corotating disks with consideration of surface roughness. *Energy*, 307, 132775. doi: 10.1016/j.energy.2024.132775.

[134] Pahlavanzadeh, M., Rusin, K., Wróblewski, W., & Rulik, S. (2025). Roughness effects on flow in Tesla turbine with parametric adjustment of porous layer model. *Physics of Fluids*, 37(1), 015139. doi:10.1063/5.0247548

[135] Pahlavanzadeh, M., Rusin, K., Wróblewski, W. (2025). Evaluation of nozzle configuration impact on flow structures and performance in Tesla turbine, International Journal of Heat and Mass Transfer 243, 126900, https://doi.org/10.1016/j.ijheatmasstransfer.2025.126900

[136] Teng, S., Li, L., Yan, C., An, D., Zhao, Y., & Xi, H. (2025). Multi-parameter experimental study of a tesla turbine applied to an Organic Rankine Cycle system for low-grade heat utilisation. *Energy Conversion and Management*, 333, 119824. doi: 10.1016/j.enconman.2025.119824

[137] Huynh, N.D., Lin, Z.-H., & Choi, D. (2021). Dynamic balanced hybridization of TENG and EMG via Tesla turbine for effectively harvesting broadband mechanical pressure. *Nano Energy*, 85, 105983. doi: 10.1016/j.nanoen.2021.105983

[138] Kiziroglou, M.E., & Yeatman, E.M. (2021). Micromechanics for energy generation. *Journal of Micromechanics and Microengineering*, 31(11), 114003. doi: 10.1088/1361-6439/ac2a52

[139] Li, C., Guo, Z., Guo, H., Bao, X., & Zhou, L. (2022). Influences of main design parameters on the aerodynamic performance of a micro-radial in flow turbine. *AIP Advances*, 12(10), 105012. doi: 10.1063/5.0090173

[140] Kosowski, K., Blekiewicz, T., Piwowarski, M., Stępień, R., Włodarski, W., Mikielewicz, J., & Kiciński, J. (2013). *Disc turbine generator with armature winding in the rotor, especially for small power plants, including hydroelectric and wind power plants*. Polish Patent PL 223125 B1 (in Polish).

[141] Kosowski, K., Blekiewicz, T., Piwowarski, M., Stępień, R., Włodarski, W., Mikielewicz, J., & Kiciński, J. (2013). *Disc turbine generator with magnetic elements in the rotor, especially for small power plants, including hydroelectric and wind power plants*. Polish Patent PL 223126 B1 (in Polish).

[142] Gad-el-Hak, M. (2006). *MEMS Introduction and Fundamentals* (2nd ed.). Taylor&Francis Group, Boca Raton, London, New York.

[143] Fréchette, L.G., Lee, C., Arslan, S.; Liu, & Y-Ch. (2003). Design of a microfabricated Rankine cycle steam turbine for power generation. *Proceedings of IMECE'03 ASME International Mechanical Engineering Congress & Exposition*, IMECE2003-42082, November 16−21, Washington, USA. doi: 10.1115/IMECE2003-42082

[144] Fréchette, L.G., Lee, C., & Arslan, S. (2004). Development of a MEMS-Based Rankine Cycle Steam Turbine for Power Generation. *4 th Workshop on Micro and Nano Technology for Power Generation & Energy Conversion Applications* (*Power MEMS'04*), (pp. 92–95), November 28−30, Kyoto, Japan.

[145] Cui, L., & Brisson, J.G. (2005). Modeling of MEMS-Type Ranking Cycle Machines. *Journal of Engineering for Gas Turbines and Power*, 127, 683−692.

[146] Maluf, N. (2000). *An Introduction of Microelectromechanical Systems Engineering*. Artech House, Inc., Boston, London.

[147] Varadan, V.K., Vinoy, K.J., & Gopalakrishnan, S. (2006). *Smart Material Systems and MEMS: Design and Development Methodologies*. John Wiley & Sons Ltd, England.

[148] Epstein, A.H. (2003). Millimeter-Scale, MEMS Gas Turbine Engines. Proceedings of ASME Turbo Expo 2003, GT-2003-38866, Power for Land, Sea, and Air Atlanta, June 16−19, Georgia, USA.

[149] Sullivan, S., Zhang, X., Ayón, A.A., & Brisson, J.G. (2001). Demonstration of a Microscale Heat Exchanger for a Silicon Micro Gas Turbine Engine. *11th International Conference on Solid-State Sensors and Actuators*, June 10–14, Munich, Germany.

[150] Müller, N., & Fréchette, L.G. (2002). Performance Analysis of Brayton and Rankine Cycle Microsystems for Portable Power Generation. *Proceedings of IMECE2002 ASME International Mechanical Engineering Congress & Exposition*, IMECE2002-39628., 513−522, November 17−22, New Orleans, Louisiana, USA. doi: 10.1115/IMECE2002-39628